

# GRAVITY-DRIVEN CONSOLIDATION OF GRANULAR SLURRIES—IMPLICATIONS FOR DEBRIS-FLOW DEPOSITION AND DEPOSIT CHARACTERISTICS

JON J. MAJOR

U.S. Geological Survey, 5400 MacArthur Boulevard, Vancouver, Washington 98661, U.S.A.  
e-mail: [jjmajor@usgs.gov](mailto:jjmajor@usgs.gov)

**ABSTRACT:** Fresh debris-flow deposits consolidate under their own weight. How quickly they consolidate (dissipate excess pore-fluid pressure and compact) affects their resistance to remobilization as well as their sedimentologic and stratigraphic characteristics. Here, analysis of small-volume ( $\sim 0.05 \text{ m}^3$ ) noncohesive debris-flow slurries and larger ( $\sim 10 \text{ m}^3$ ) experimental debris-flow deposits reveals the nature, rate, and magnitude of consolidation of typical debris-flow deposits.

A simple, linear, one-dimensional model describing the diffusion of excess pore-fluid pressure satisfactorily approximates the overall timing and magnitude of consolidation of noncohesive debris-flow deposits. The model and measurements of pore-fluid pressure demonstrate that changes in fluid pressure and effective stress evolve upward from the base of a deposit, and show that hydraulic diffusivities of muddy slurries containing about 5 to 50 wt% mud are remarkably similar, about  $10^{-6}$ – $10^{-7} \text{ m}^2/\text{s}$ . By comparison, sandy-gravel debris-flow deposits containing  $<2$  wt% mud have higher hydraulic diffusivities,  $\sim 10^{-4} \text{ m}^2/\text{s}$ . Pore-fluid seepage across a permeable basal boundary accelerates consolidation response time in the lower stratum compared to that over a no-flow boundary. However, changes in sediment fabric resulting from porosity changes alter hydraulic properties of basal debris and retard expected decay of fluid pressure immediately above the bed. This result suggests that fluid infiltration to the substrate does not contribute significantly toward debris-flow deposition.

Low hydraulic diffusivities promote high and persistent pore-fluid pressure in debris flows, key factors enhancing mobilization. Elsewhere, pore-fluid pressures nearly sufficient to liquefy debris have been shown to persist through transit and deposition. Here, I show that significant dissipation of such fluid pressure is restricted to postdepositional consolidation. Therefore, neither uniform decay of excess pore-fluid pressure nor intrinsic viscoplastic yield strength explain debris-flow deposition. Instead, debris-flow deposition results from friction concentrated along flow margins where high pore-fluid pressures are absent. Sustained high pore-fluid pressure following deposition fosters deposit remobilization, which can mute or obliterate stratigraphic evidence for multiple events. A thick deposit of homogeneous, poorly sorted debris can result from mingling of soft deposits and recurrent surges rather than from a single flow wave if deposit consolidation time greatly exceeds typical sediment emplacement times.

## INTRODUCTION

Pore-fluid pressure strongly influences the initiation, transport, and deposition of debris flows (Iverson and LaHusen 1989; Eckersley 1990; Takahashi 1991; Iverson 1997a, 1997b; Iverson et al. 1997; Spence and Guymer 1997; Mohrig et al. 1998; Major and Iverson 1999). Moreover, high pore-fluid pressure persists after deposition. Major and Iverson (1999) show that pore-fluid pressures nearly equal to the unit weight of saturated debris, which developed during flow mobilization, persisted during deceleration and deposition of large, experimental debris flows. Dissipation times of elevated pore-fluid pressures measured at the bases of those deposits varied greatly, and depended chiefly upon debris composition. Fluid pressure in excess of hydrostatic pressure dissipated within tens of seconds to several minutes in sandy-gravel deposits that contained  $<2$  wt% mud ( $<63 \mu\text{m}$ ) (Fig. 1A, B; Table 1). In contrast, elevated pore-fluid pressures in comparably thick loamy-gravel deposits that contained about 2–4 wt% mud dissipated over several hours (Fig. 1C, D; Table 1). Laboratory measurements of fluid pressures in small volumes of static muddy debris show similar results (Hampton 1979; Pierson 1981).

Persistent, postdepositional, excess pore-fluid pressure is not unique to experimental debris flows. Descriptions of freshly deposited debris and of measured stratigraphic sequences yield the impression that excess pore-fluid pressure persists in many natural debris-flow deposits as well. Evidence of persistent excess fluid pres-

sure in natural debris-flow deposits includes: (1) fresh deposits having margins that are firm but interiors that are too weak to walk on for days to weeks (e.g., Fryxell and Horberg 1943; Curry 1966; Broscoe and Thomson 1969); (2) soft-sediment deformation at the surface of, and within stratigraphic sequences of, debris-flow deposits (e.g., Fryxell and Horberg 1943; Jahns 1949; Postma 1983; Major et al. 1996); (3) development of seeps and springs on deposit surfaces (e.g., DeGraff 1994); (4) translation of waves through deposited debris (e.g., Sharp and Nobles 1953; Morton and Campbell 1974; Wasson 1978; Costa and Williams 1984); and (5) relatively easy remobilization of debris by subsequent surges or flows (e.g., Sharp and Nobles 1953; Costa and Williams 1984).

Sustained excess pore-fluid pressure can affect the sedimentologic and stratigraphic characteristics of debris-flow deposits. Excess pore-fluid pressure diminishes the frictional strength of sedimentary deposits. When excess pore-fluid pressure is high, sedimentary deposits are weak and they can fail under subsequent loading. Failure can lead to soft-sediment deformation structures such as convolute bedding, flame structures, and fluidization pipes (e.g., Collinson and Thompson 1989). However, such structures need not form when sedimentary deposits are disturbed. Instead, stratigraphic contact between sedimentary deposits may simply be obscured, especially if deposits have similar textures.

Obscure contacts among debris-flow deposits can cloud correct interpretation of depositional process. Debris-flow deposits are commonly interpreted to result from a sudden “freezing” of flow that occurs when driving stress can no longer overcome resisting stresses (e.g., Johnson 1970, 1984; Takahashi 1991). Sudden “freezing” of flow is invoked to explain the poorly sorted, commonly matrix-supported character of many debris-flow deposits (e.g., Middleton and Hampton 1976; Lowe 1982; Cas and Landis 1987; Ghibaudo 1992; Kim et al. 1995). Recent field studies have suggested, however, that a poorly sorted matrix-supported deposit may result from incremental sedimentation (Vallance and Scott 1997), and large-scale flume experiments have demonstrated that a homogeneous, massive-textured, poorly sorted deposit can result from incremental accretion of surges of debris rather than from simple “freezing” of a single surge (Major 1997). Lack of stratigraphic evidence for multiple episodes of deposition can result from disturbance of previously deposited debris (Major 1997). Disturbance of temporally related debris-flow deposits and clouding of stratigraphic contacts depends, in part, on timescale relations between postdepositional dissipation of excess pore-fluid pressure and return periods of sediment emplacement.

Complete understanding of the depositional process, and the potential for rapid postdepositional modification, of coarse-grained mass flows has been hampered by a lack of replicable data that document the temporal evolution of pore-fluid pressure in debris-flow slurries. Previous investigations of fluid pressures in static debris-flow slurries (e.g., Pierson 1981) have not interpreted temporal changes with an appropriate consolidation theory, nor have they identified the significance of fluid-pressure changes with respect to depositional process or deposit character. In this paper, I discuss a suite of experiments that examine fluid-pressure evolution in small-volume debris slurries and larger debris-flow deposits that consolidate under their own weight. The experiments provide insight on the pore-fluid hydraulics and consolidation of liquefied granular (noncolloidal) debris. Moreover, these experiments, in conjunction with those reported by Major and Iverson (1999), aid our understanding of the mechanics of debris-flow deposition, and they provide a link between postdepositional consolidation and deposit characteristics.

## CONSOLIDATION—CONCEPTUAL PROCESS AND ONE-DIMENSIONAL THEORY

Consolidation refers to the time-dependent compaction of a fluid-filled porous medium under load. A sedimentary deposit, which can be visualized as a skeleton of solid particles enclosing connected voids that are filled with water and air, is the most common naturally occurring fluid-filled porous medium. Sedimentary deposits consolidate in response to a load applied externally at their surface; however, they may consolidate in response to gravitational body force in the absence of a surface

TABLE 1.—Grain-size characteristics and representative hydraulic properties of sediment (&lt;32 mm diameter) used in debris-flow-flume and consolidation-tank experiments (cf. Major 1997; Major et al. 1997)

Deposit Number	Median Grain Diameter (mm)	Mean Grain Diameter (mm)	Sorting Coefficient (phi units)	Skewness Coefficient (phi units)	Weight % Gravel	Weight % Sand	Weight % Silt	Weight % Clay	Permeability† Max./Min. (m <sup>2</sup> )	Porosity† Max./Min.
040793 <sup>1</sup>	4.2	2.9	2.3	0.3	60.6	38	1.4 <sup>2</sup>	—	5 × 10 <sup>-10/2</sup> × 10 <sup>-12</sup>	0.37/0.26
040893 <sup>1</sup>	7.4	3.7	2.4	0.5	63.3	35.6	1.1 <sup>2</sup>	—	—	—
	3.9	2.6	2.3	0.3	57.6	40.6	1.8 <sup>2</sup>	—	—	—
	5.3	3.2	2.3	0.4	64.6	33.8	1.6 <sup>2</sup>	—	—	—
	5.2	3.1	2.3	0.4	62.8	35.6	1.6 <sup>2</sup>	—	—	—
052694 <sup>3</sup>	0.4	0.5	1.5	-0.3	13.5	84.4	1.9	0.2	4 × 10 <sup>-11/4</sup> × 10 <sup>-12</sup>	0.41/0.34
	0.3	0.4	1.8	-0.3	12.8	83.3	3.6	0.3	—	—
	0.4	0.6	2.1	-0.3	7.6	76.1	3.9	0.4	—	—
	0.4	0.6	2.0	-0.3	19.2	76.7	3.7	0.4	—	—
083194 <sup>3</sup>	2.3	2.5	2.6	0.0	51.8	46.6	1.5	0.1	—	—
	8.1	4.3	2.5	0.5	61.8	36.8	1.2	0.2	—	—
	3.1	2.7	2.7	0.1	54.2	43.8	1.8	0.2	—	—
	1.6	2	2.8	-0.05	48	49.9	1.9	0.2	—	—
MSH	0.5	0.5	3.8	0.05	29.6	50.3	18.3	1.8	3 × 10 <sup>-11/2</sup> × 10 <sup>-14</sup>	0.50/0.33
OSC	0.05	0.03	7.3	0.1	31.4	15.9	35.5	17.2	2 × 10 <sup>-11/5</sup> × 10 <sup>-15</sup>	0.60/0.44

Median grain diameter calculated from Inman (1952); mean grain diameter, sorting coefficient, and skewness coefficient calculated from Folk (1984); MSH is Mount St. Helens debris; OSC is Oseola Mudflow debris.

† Obtained from modified compaction-permeameter and triaxial-cell tests (see Major et al. 1997). Max/min represent maximum and minimum values measured.

<sup>1</sup> Pore-fluid pressures were not measured in these deposits. However, the sandy gravel used as source debris in these experiments was similar to that of deposits 041994 and 042194 in which pore-fluid pressures were measured.

<sup>2</sup> Weight percent of silt and clay combined.

<sup>3</sup> These and similar deposits could be variously classified as muddy sandy gravel to gravely sand (Folk 1984). For simplicity I refer to deposits containing >2% mud as loamy gravel regardless of the ratio of sand to mud or the percentage of gravel.

load. Regardless of how a load is applied, the degree to which sediment consolidates and the response time of consolidation are related to the physical properties of the sediment grains, the pore fluid, and the bulk properties of the sedimentary deposit. There are three possible ways for water-saturated sediment to consolidate: (1) the water that fills the pore space can compress; (2) the sediment grains can deform; or (3) the grains can rearrange themselves into a more closely packed configuration by squeezing water out of the pores and closing pore space. Natural near-surface stresses as well as stresses imposed during engineering projects are sufficiently small that pore water can be considered incompressible. Although some elastic or plastic strain occurs along grain contacts in response to loading, compaction of saturated sedimentary deposits induced by grain rearrangement is much more important than compaction induced by grain deformation. Therefore, one-dimensional consolidation of saturated sediment occurs only if water can drain from the sediment and voids can shrink.

Consolidation settlement refers to the vertical displacement that occurs as sediment compacts. If sediment is laterally constrained, vertical settlement of a saturated deposit can occur only if pore fluid can escape. If there is significant lateral strain, some vertical settlement occurs immediately after loading without loss of pore fluid. Vertical settlement is most easily quantified by measuring surface displacement with respect to an initial elevation. One measure of the magnitude of consolidation is the temporal change of surface displacement.

Traditional consolidation analyses examine the response that follows application of an external surface load, and they typically focus on consolidation of clay-rich sediment (e.g., Terzaghi 1923, 1943; Lambe and Whitman 1969). However, gravitational, rather than surface, loading can be important, and a few studies have considered the gravitational, or self-weight, consolidation problem (e.g., Gibson et al. 1967; Lee and Sills 1981; Been and Sills 1981; Audet and McConnell 1992; Toorman 1996; Fox and Berles 1997). Gravity-driven consolidation occurs in sediment not in equilibrium with the gravitational stress field; for example, in lakes or estuaries owing to continuous sedimentation; in hydraulic fills that are not artificially compacted; in large sedimentary basins; in sludges; and in rapidly deposited slurries.

### Basic Concepts

**Fluid Pressure and Total Stress.**—The pressure, or normal stress, acting on any plane in a mass of saturated sediment depends on the fluid that fills the pore space and the solid grains that make up the sediment skeleton. Thus, we must distinguish the fluid pressure (exerted only by the fluid), the skeleton pressure or intergranular stress (exerted only by the solids), and the total stress (which reflects a combination of the fluid and skeleton pressure). The total stress is equivalent to the stress transmitted normal to a plane if the sediment is imagined to be composed of a solid, single-phase material.

Fluid pressure and total stress within saturated sediment vary with depth. Consider a one-dimensional, water-saturated sedimentary deposit in which the vertical coordinate direction,  $z$ , is defined positive upwards (Fig. 2). If intergranular contacts carry all of the weight of the solids and if water statically fills the pore space among the grains, then the hydrostatic pressure  $P_h$  of a column of water extending from the deposit surface to a depth  $H - z$  is given by

$$P_h = \rho_w g(H - z) \quad (1)$$

where  $\rho_w$  is the density of water,  $g$  is the gravitational acceleration in the coordinate direction, and  $H$  is the coordinate value identifying the deposit surface (Fig. 2). The total stress,  $\sigma_{zz}$ , of a column of water-saturated sediment extending from the deposit surface to the same depth is given by

$$\sigma_{zz} = -\rho_t g(H - z) \quad (2)$$

where  $\rho_t$  is the total mass density of the water-saturated debris. (The negative sign follows the convention that total stress is defined negative in compression, whereas fluid pressure is defined positive.) The total mass density can be written in terms of water density  $\rho_w$ , grain density  $\rho_s$ , and porosity  $\phi$  as  $\rho_t = \rho_w \phi + \rho_s(1 - \phi)$ . Substitution of this definition into Eq 2, and some minor manipulation, leads to

$$\sigma_{zz} = -[\rho_w + (\rho_s - \rho_w)(1 - \phi)]g(H - z) \quad (3)$$

This expression shows that total stress in a column of water-saturated debris depends on the weight of the column of overlying water plus the buoyant weight of the column of overlying solids. Depth dependence of stress and fluid pressure distinguishes gravity-driven consolidation from conventional consolidation driven by applied surface loads.

A water-saturated deposit becomes packed into a more stable configuration under load. If the load is added rapidly, pore-fluid pressure changes. Pore-fluid pressure changes because the water that fills the pore space is incompressible and it resists particle rearrangement; that resistance leads to a temporary increase in the fluid pressure. After rapid loading, the pressure in a column of water extending from the deposit surface to some depth is greater than hydrostatic, and can be written as  $P_t$ ,

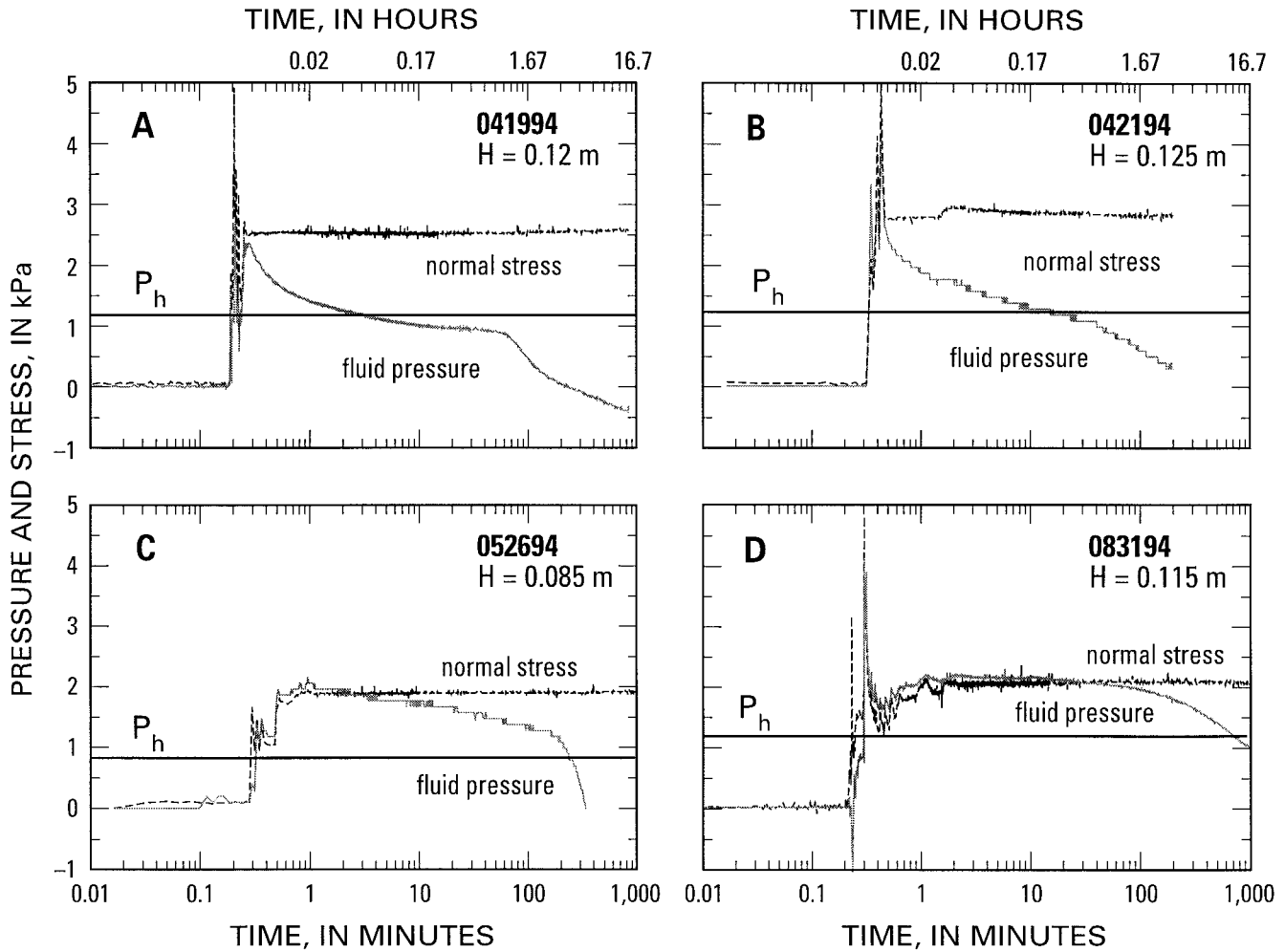


FIG. 1.—Representative measurements of basal fluid pressure and total basal normal stress in debris-flow deposits at the U.S. Geological Survey debris-flow flume (Iverson et al. 1992; Major 1997; Major and Iverson 1999). All data are for deposits having volumes that range from 8.5 to 10 m<sup>3</sup>. Experimental debris included **A, B**) sandy gravel containing <2 wt% mud (silt + clay) and **C, D**) loamy gravel containing 2–4 wt% mud (C, D). See Table 1 for debris characteristics. Progressive abrupt peaks in both fluid pressure and normal stress reflect loading of deposits by successive surge waves (cf. Major and Iverson 1999).  $H$  is deposit thickness. The hydrostatic fluid pressure ( $P_h$ ) at the base of the deposit is shown. For details regarding measurement methods, see Major and Iverson (1999).

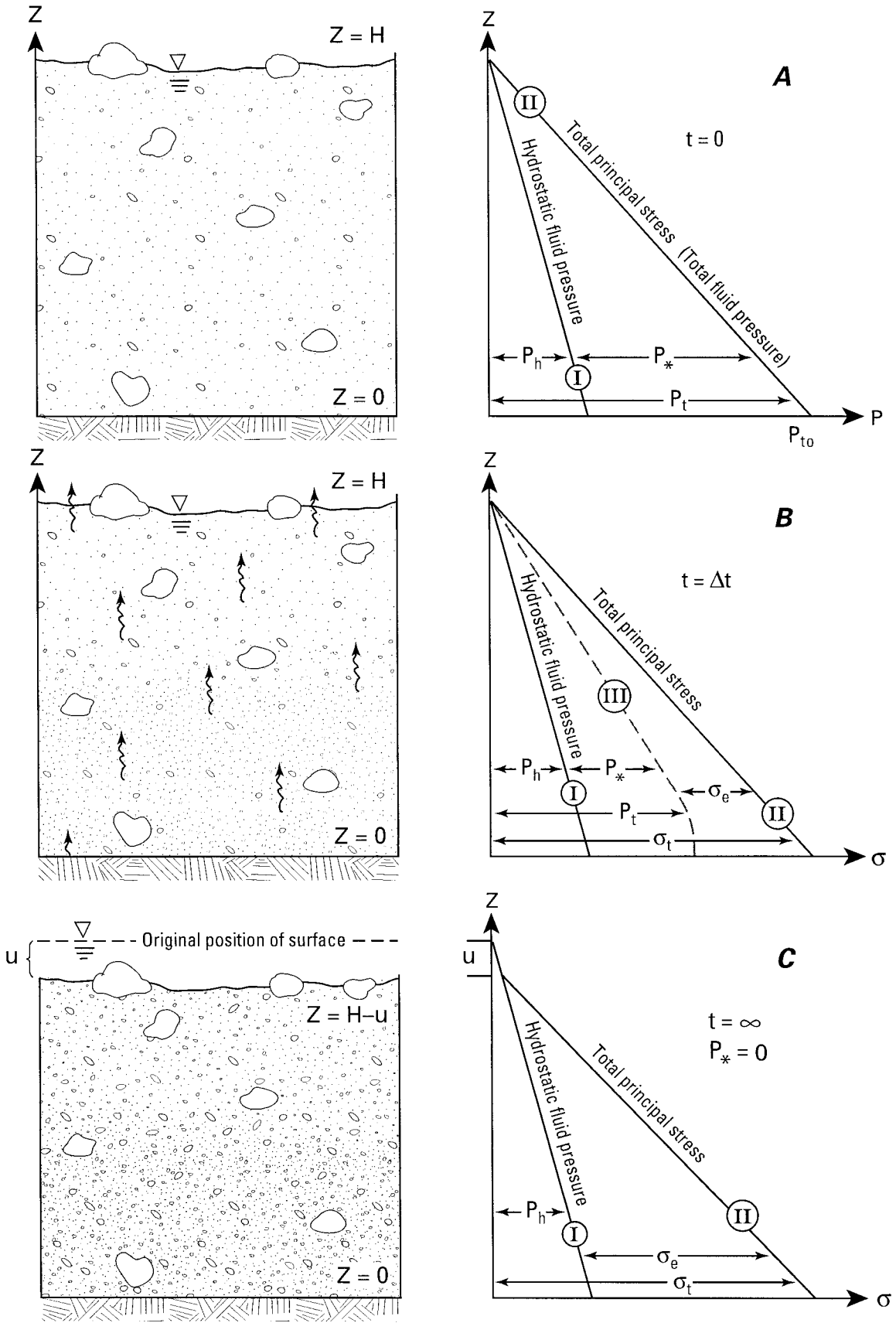
$= P_h + P_*$ , where  $P_t$  is the total fluid pressure and  $P_*$  is the excess, or nonequilibrium, fluid pressure (Fig. 2A). The initial increase in pore-fluid pressure is equal to the change in total stress. When pore-fluid pressure is greater than hydrostatic, a fluid-pressure gradient is established, which results in transient fluid flow toward a freely draining boundary. As excess pore-fluid pressure dissipates, load is transferred from the pore fluid to intergranular contacts, grain packing changes, and the deposit consolidates. Therefore, another measure of consolidation is the temporal response of pore-fluid pressure to sudden load (Fig. 2B).

If intergranular contacts are thoroughly disrupted under load, or if a sediment mass is deposited so rapidly that intergranular contacts are very poorly established, then the pore fluid may bear the entire weight of the solid grains temporarily, and the mass is said to be liquefied. In that case, the total fluid pressure equals the total normal stress. Thus,  $P_t = -\sigma_{zz}$ , or

$$P_t = [\rho_w + (\rho_s - \rho_w)(1 - \phi)]g(H - z) \quad (4)$$

This expression can be recast as

FIG. 2.—Definition sketch of element geometry, fluid pressures, and stress fields for one-dimensional gravity-driven consolidation of a saturated slurry overlying an impermeable bed. The coordinate system is defined positive upwards:  $z = 0$  at the bed;  $z = H$  at the slurry surface.  $P_h$  is hydrostatic fluid pressure;  $P_*$  is fluid pressure in excess of hydrostatic;  $P_t$  is the total fluid pressure; and  $P_{t0}$  is the initial value of the total fluid pressure at the base of the slurry.  $\sigma_t$  is the total normal stress,  $\sigma_e$  is the effective normal stress, and  $u$  represents settlement of the deposit surface. Mathematical definitions of these quantities are given in the text. **A**) Initial state of dilated, liquefied slurry. The total fluid pressure is equal to the unit weight of the debris. A probe measuring fluid pressure at any depth would measure values along line II. **B**) Consolidation state at time  $\Delta t$ . Settling of buoyant grains generates excess pore-fluid pressure that dissipates through Darcian seepage. A probe measuring the fluid pressure at any depth would measure values along line III. As excess pore-fluid pressure dissipates, changes occur in grain packing, and line III shifts left. The excess pore-fluid pressure is defined by the width of the region between the profiles of hydrostatic pressure (I) and total fluid pressure (III). The total stress remains constant during consolidation, and the effective intergranular stress represents the region between the profiles of total fluid pressure (III) and total stress (II). As excess pore-fluid pressure dissipates, effective stress increases. **C**) Post-consolidation (drained) state. Excess pore-fluid pressure has dissipated. A probe would measure hydrostatic pore-fluid pressure along line I at all depths. The effective stress is defined by the width of the region between lines I and II. Note that the deposit surface settles by an amount  $u$  in response to changes in grain packing.



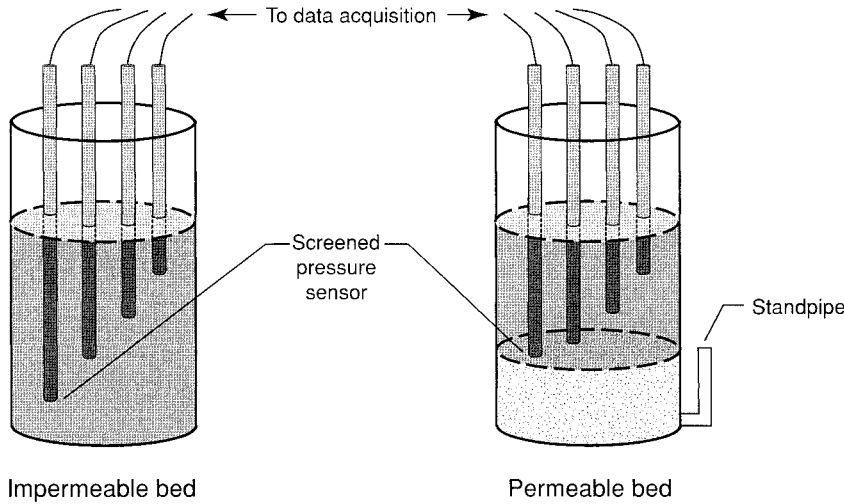


FIG. 3.—Schematic diagram of consolidation tank. Screened pressure probes are suspended in the tank. After mixing, debris slurry is poured rapidly into the tank. Saturation of permeable bed is maintained by a fluid-filled standpipe.

$$P_t = \rho_w g(H - z) + (\rho_s - \rho_w)(1 - \phi)g(H - z) \quad (5)$$

or

$$P_t = P_h + P_* \quad (6)$$

Thus, when a sedimentary deposit is liquefied, gravity induces a downward flux of sediment toward the bed, and the excess fluid pressure is equal to the buoyant unit weight of the sediment (Fig. 2A),

$$P_* = (\rho_s - \rho_w)(1 - \phi)g(H - z) \quad (7)$$

**Effective Stress.**—The total stress in a column of water-saturated sediment can be partitioned into components that describe the state of the fluid pressure and the intergranular stress. Such partitioning of stresses leads to the concept of effective stress, a concept recognized by Lyell as early as the late 1800s (Skempton 1960), but not explicitly stated until Terzaghi (1923, 1943) proposed a simple theoretical framework for consolidation. The mathematical definition of effective stress,  $\sigma_{zz}^e$ , most useful for describing volume deformation in granular materials is given by (e.g., Terzaghi 1923, 1943; Jaeger and Cook 1979)

$$\sigma_{zz}^e = \sigma_{zz} + P_t \quad (8)$$

(The difference between the total normal stress,  $\sigma_{zz}^e$ , and the total fluid pressure,  $P_t$ , appears additive, rather than subtractive, because  $\sigma_{zz}$  is defined negative in compression whereas  $P_t$  is defined positive.) It is illuminating to partition the total stress in this manner. In saturated sediment, water pervasively fills the pores and the fluid pressure acts in every direction with equal intensity. Simply increasing the fluid pressure does not cause volume change. This can be illustrated in the following thought experiment. Consider a closed container of laterally confined saturated sediment from which pore fluid cannot escape. If a weight is added instantly to the surface, the total stress within the deposit increases. In response to this stress change, sediment grains attempt to pack closer together. However, because water cannot escape and because it is incompressible, particle rearrangement cannot occur. As a result, intergranular stresses cannot change, the sediment cannot compact, and the total fluid pressure increases by an amount equal to the total stress change. Now consider the case in which pore fluid escapes. Suppose that the surface load is applied so slowly that pore fluid is expelled continuously and the fluid pressure within the deposit remains essentially hydrostatic. In this case, grain packing changes gradually by slowly squeezing out the pore fluid, and the mass compacts. This time total stress within the mass changed, but fluid pressure remained unchanged, and the sediment consolidated. Consolidation therefore occurred in response to changes in the intergranular, or effective, stress. In a static, saturated deposit, the vertical effective stress equals the buoyant unit weight of the sediment (cf. Eqs 3 and 8; Fig. 2C).

Terzaghi originally coupled deposit deformation to effective stress through a linearly elastic rheology, and restricted the theory to a state of infinitesimal strain. Subsequent sophisticated refinements of consolidation theory include coupling of strain to both sediment stress and fluid pressure, consideration of nonlinear and nonelastic sediment rheology, and accommodation of large strains (e.g., Biot 1941; Davis and Raymond 1965; Gibson et al. 1967; Carter et al. 1979; Schiffman et al. 1984; Fox and Berles 1997).

In this paper, I focus on gravity-driven consolidation of dominantly sandy, non-cohesive slurries at low effective stresses ( $\leq 20$  kPa). Self-weight consolidation of these types of slurries under low effective stresses can occur following sudden deposition by a debris flow, as demonstrated by the temporal response of fluid pressure at the base of several flume deposits (Fig. 1). I examine consolidation of debris-flow slurries with the aid of Terzaghi's simple, linear, one-dimensional model, but I incorporate a gravitational body force. I take this admittedly simplified approach because: (1) sandy sediment is much less compressible than clay (e.g., Lambe and Whitman 1969, p. 297); (2) surface settlement of flume deposits was small relative to deposit thickness (vertical strain  $< 5$  percent); (3) debris-flow deposits typically are much broader than they are thick, thus consolidation is dominantly one-dimensional; and (4) a linear model provides a convenient starting point that avoids complications resulting from large changes in porosity.

### One-Dimensional Consolidation Theory

**Theoretical Expression.**—Expressions for the diffusion of excess fluid pressure provide the basis for analysis of quasistatic consolidation (e.g., Terzaghi 1943; Gambolati 1973; Sills 1975; Lambe and Whitman 1969; Craig 1992). An expression for one-dimensional linear consolidation in terms of diffusion of excess fluid pressure,  $P_*$ , is given by

$$\frac{\partial P_*}{\partial t} - D \frac{\partial^2 P_*}{\partial z^2} = 0 \quad (9)$$

where the diffusion coefficient  $D = kE_s/\mu$ ;  $E_s$  is the constrained modulus, a measure of the bulk stiffness of a porous medium under confined uniaxial strain (reciprocal of compressibility);  $k$  is the hydraulic permeability of the porous medium; and  $\mu$  is the dynamic viscosity of the pore fluid. Derivation of this expression can be found in many standard texts (e.g., Terzaghi 1943; Lambe and Whitman 1969; Craig 1992). Development of this linear diffusion equation is predicated on several key assumptions: (i) bulk compressibility of a sedimentary deposit is more important than the compressibility of water or sediment grains; (ii) strain is uniaxial,  $\epsilon_{zz} \neq \epsilon_{xx} = \epsilon_{yy} = 0$ ; (iii) strain is linearly related to vertical effective stress,  $\sigma_{zz}^e$ , by  $\epsilon_{zz} = (1/E_c)\sigma_{zz}^e$ ; (iv) specific fluid discharge,  $q$ , is described by Darcy's law, which can be written in terms of excess fluid pressure as  $q = -(k/\mu)(\partial P_*/\partial z)$ ; (v) solids are uniformly distributed throughout the deposit; and (vi) the total vertical stress is time invariant. Assumptions i-v provide reasonable first-order approximations describing conditions in wide, thin deposits of saturated, poorly sorted sandy debris subject to low-magnitude stresses. Assumption vi reasonably describes the state of total vertical stress, as measured at the base of several debris-flow deposits (Fig. 1). The diffusion equation (Eq 9) is applicable to both externally driven and gravity-driven consolidation. The primary difference between those two styles of consolidation rests in the state of stress and initial fluid pressure that develop following instantaneous loading.

**Initial and Boundary Conditions.**—Appropriate initial and boundary conditions are needed to solve Eq 9. An initial fluid pressure can be approximated if we assume that loading is rapid relative to transient fluid flow. This assumption is appropriate for rapidly deposited slurries; fluid pressures in flume deposits remained elevated for a few seconds to several tens of minutes following deposition (Fig. 1; Major

TABLE 2.—Initial fluid pressure and estimated initial porosity in debris-flow-flume deposits and tank slurries

Deposit Number§	Domain Level z (m)	$P_t$ (Pa)	$P_*$ (Pa)	Depth (m)	Initial Porosity $\phi^\dagger$	$1-\phi$	$P_t/P_h$	Mean Surface $\phi^\ddagger$	Volume % Solids**
041994	0	2350	1175	0.12	0.39	0.61	2.0	0.27–0.29	
042194	0	2550	1275	0.13	0.39	0.61	2.0	0.29	
052694	0	1760	975	0.08	0.25	0.75	2.3	0.33–0.38	67
083194	0	2550	1375	0.12	0.29	0.71	2.2	0.30	67
C4	.69	4700	2350	0.24	0.39	0.61	2.0		68
flume debris	.54	8040	4220	0.39	0.33	0.67	2.1		
	.37	11760	6275	0.56	0.31	0.69	2.1		
C5	.68	4310	2250	0.21	0.34	0.66	2.1		67
flume debris	.57	6615	3480	0.32	0.33	0.67	2.1		
	.39	10290	5390	0.50	0.33	0.67	2.1		
C6	.42	4115	2250	0.19	0.27	0.73	2.3		65
flume debris	.20	8625	4610	0.41	0.30	0.70	2.2		
	.03	11960	6275	0.58	0.33	0.67	2.1		
C7	.49	1960	980	0.10	0.39	0.61	2.0		67
flume debris	.23	7640	4115	0.36	0.29	0.71	2.2		
	.01	11960	6275	0.58	0.33	0.67	2.1		
C8	.45	2840	1565	0.13	0.26	0.74	2.2		70
flume debris	.25	7050	3815	0.33	0.29	0.71	2.2		
	.01	11760	6075	0.58	0.35	0.65	2.1		
C9	.50	2350	1175	0.12	0.39	0.61	2.0		68
flume debris	.29	6740	3500	0.33	0.34	0.66	2.1		
	.01	12940	6960	0.61	0.29	0.71	2.2		
C10	.45	2250	1175	0.11	0.35	0.65	2.1		69
flume debris	.22	7350	4020	0.34	0.27	0.73	2.2		
	.00	11560	6075	0.56	0.33	0.67	2.1		
C11	.49	3040	1375	0.17	0.50	0.50	1.8		52
OSC	.25	7400	3380	0.41	0.49	0.51	1.8		
	.02	11560	5290	0.64	0.49	0.51	1.8		
C12	.70	3800	1745	0.21	0.49	0.51	1.8		58
OSC	.40	9900	4900	0.51	0.41	0.59	2.0		
C13	.74	4200	2045	0.22	0.43	0.57	2.0		58
OSC	.60	7100	3575	0.36	0.39	0.61	2.0		
	.44	10125	5030	0.52	0.40	0.60	2.0		
	.06	17250	8430	0.90	0.42	0.58	2.0		
C14	.28	7645	3825	0.39	0.39	0.61	2.0		71
MSH	.19	10000	5300	0.48	0.32	0.68	2.1		
	.12	11470	6080	0.55	0.32	0.68	2.1		
	.00	12940	6375	0.67	0.41	0.59	2.0		
C15***	.58	1695	615	0.11	0.65	0.35	1.6		61
OSC	.37	6225	3100	0.32	0.40	0.60	2.0		
	.19	9600	4700	0.50	0.42	0.58	2.0		
	.07	11960	5880	0.62	0.41	0.59	2.0		
C16	.88	3725	2060	0.17	0.25	0.75	2.2		68
MSH	.68	7250	3625	0.37	0.39	0.61	2.0		
	.40	13230	6860	0.65	0.35	0.65	2.1		
	.08	20290	10785	0.97	0.31	0.69	2.1		
C17	.80	3730	1870	0.19	0.39	0.61	2.0		62
MSH	.60	7550	3725	0.39	0.41	0.59	2.0		
	.43	11660	6175	0.56	0.32	0.68	2.1		
	.10	18720	10000	0.89	0.31	0.69	2.2		
C18	.57	2550	1275	0.13	0.39	0.61	2.0		69
MSH	.39	6470	3530	0.30	0.27	0.73	2.2		
	.18	10975	5975	0.51	0.28	0.72	2.2		
	.01	14600	7940	0.68	0.28	0.72	2.2		

$\phi$ , porosity;  $1-\phi$ , solids fraction;  $P_t$ , total fluid pressure;  $P_*$ , excess fluid pressure;  $P_h$ , hydrostatic fluid pressure.

§ Flume debris is from deposit 052694; C indicates tank consolidation experiment; other abbreviations, see Table 1.

† Obtained by solving Eq 7 for  $\phi$ ; assumes that  $\gamma_s - \gamma_w = 16170 \text{ N/m}^3$ ,  $\gamma = \rho g$ .

‡ From Iverson (1997a).

\*\* Estimated from sampling slurry after mixing.

\*\*\* Apparently low total fluid pressure and excessively large estimated porosity indicate that slurry was not liquefied at this depth.

and Iverson 1999). During instantaneously undrained loading, volume change is negligible. Thus, no vertical strain occurs and  $\epsilon_{zz} = 0$  at  $t = 0$ . As a result, the effective stress is initially negligible ( $\epsilon_{zz} \propto \sigma_{zz}^e$ ), the pore fluid bears the unit weight of the saturated debris, and  $-\sigma_{zz} = P_t$  (cf. Eq 8). Therefore, a rapidly deposited saturated slurry that is instantaneously undrained should be liquefied temporarily, and the total fluid pressure should approach the liquefaction pressure described by Eq 5. Fluid pressures of this magnitude have been measured following deposition of experimental debris flows (Fig. 1; Major and Iverson 1999). The nonhydrostatic component of that liquefaction pressure, described by Eq 7, establishes the initial-condition fluid pressure.

The boundary conditions considered here are simple. Fluid is allowed to drain freely across the upper boundary; thus  $P_* = 0$  at  $z = H$  (Fig. 2). Two different basal boundary conditions are investigated (Fig. 3). In one case, no fluid flow is permitted across the basal boundary; therefore,  $\partial P_*/\partial z = 0$  at  $z = 0$ . In the second case, fluid is allowed to drain freely across the basal boundary; thus  $P_* = 0$  at  $z = 0$ .

**Analytical Solutions.**—Subject to the appropriate boundary and initial conditions described, the transient excess-fluid-pressure field for a no-flux basal boundary condition is given by (Carslaw and Jaeger 1959, p. 97):

$$P_* = 8P_{*0} \sum_{n=0}^{\infty} \frac{1}{(2n+1)^2 \pi^2} \cos(\lambda_n z) e^{-\lambda_n^2 D t} \quad (10)$$

where  $P_{*0}$  represents the initial excess pore-fluid pressure at  $z = 0$  (cf. Eq 7), and  $\lambda_n$  are eigenvalues. Transient behavior of other quantities of interest, such as effective stress and surface displacement, are obtained from relations between excess fluid pressure, total stress, and effective stress (Eqs 6 and 8), effective stress and vertical strain (as specified above), and vertical strain and displacement ( $\epsilon_{zz} = \partial u_z / \partial z$ , where  $u_z$  represents the solids displacement in the coordinate direction). An expression for the transient change of vertical effective stress is given by

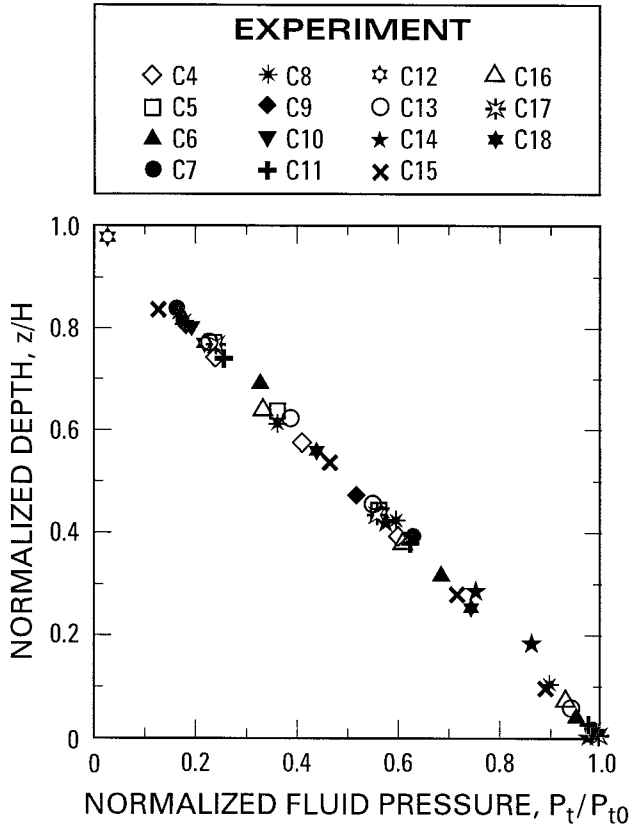


FIG. 4.—Initial profiles of total fluid pressure measured in tank experiments. Position within the slurry ( $z$ ) is normalized by initial slurry depth ( $H$ ). Fluid pressure is normalized by the initial value of fluid pressure at the base of the slurry. Open symbols are impermeable-bed experiments; solid symbols are permeable-bed experiments.

$$\sigma_{zz}^e = -(\rho_s - \rho_w)(1 - \phi) \times g \left[ (H - z) - 8H \sum_{n=0}^{\infty} \frac{1}{(2n + 1)^2 \pi^2} \cos(\lambda_n z) e^{-\lambda_n^2 D t} \right] \quad (11)$$

An expression for displacement results from the relationship between effective stress and strain, from integrating the definition of infinitesimal strain, and from imposing the condition that no displacement occurs at the basal boundary ( $u(0, t) = 0$ ). Time-dependent surface displacement is obtained by setting  $z = H$ , which yields

$$u_H = -\frac{1}{E_c} (\rho_s - \rho_w)(1 - \phi) \times g \left[ \frac{H^2}{2} - 8H \sum_{n=0}^{\infty} \frac{1}{(2n + 1)^2 \pi^2} \frac{\sin(\lambda_n H)}{\lambda_n} e^{-\lambda_n^2 D t} \right] \quad (12)$$

#### EXPERIMENTAL ANALYSIS OF CONSOLIDATION

I conducted replicate tank experiments, in which noncohesive slurries overlying an impermeable bed were allowed to consolidate under their own weight, in order to test the transient behaviors predicted by Eqs 10–12. I also used slurries overlying a permeable bed. Expressions describing transient field behavior with a drained basal boundary are given in Appendix 1.

I used a smooth-walled, 0.25-m-diameter cylindrical aluminum tank approximately 1 m tall filled with 30 to 50 l of slurried sediment (Fig. 3). The bottom of the tank was sealed in some experiments to achieve an impermeable bed. In other experiments, the tank was packed with a saturated bed of permeable 2–16-mm-diameter pea gravel or compacted, 0.25–2-mm sand (Fig. 3). Permeabilities of sub-

strate sediment exceeded slurry permeabilities by a factor of 10 or more (Major et al. 1997). Substrate sediment was covered with thin porous cloth to maintain the sharp permeability contrast at the slurry boundary at a fixed position. Connecting the tank to an open, water-filled standpipe that extended as high as the permeable substrate achieved the appropriate zero-pressure basal boundary condition (Fig. 3).

Experimental slurries consisted of poorly sorted mixtures of gravel (to several millimeters in diameter), sand, and mud (silt plus clay  $< 63 \mu\text{m}$ ) (Table 1). Sediment came from three sources: loamy gravel used during experiments at the U.S. Geological Survey debris-flow flume (cf. Iverson et al. 1992; Iverson and LaHusen 1993; Major 1997; Major et al. 1997; Major and Iverson 1999); the clay-rich Osceola Mudflow deposit from Mount Rainier, Washington (Vallance and Scott 1997); and the 1980 North Fork Toutle River debris-flow deposit from Mount St. Helens, Washington (Scott 1988). These sediments have a range of clay contents and other properties that span the physical characteristics of many debris flows (Major et al. 1997).

Experimental procedure involved (1) blending approximately 50 l of sediment with tap water in a portable mixer until the mixture attained the consistency of wet concrete, (2) pouring the slurry into the tank, (3) measuring pore-fluid pressure at various levels within the slurry, and (4) tracking surface displacement. The water content and volume fraction of solids of each slurry were determined after mixing (Table 2). Local fluid pressures, measured by suspended, screened pressure probes (Fig. 3), were logged directly by computer. Excess fluid pressure was determined by subtracting hydrostatic fluid pressure from measured total fluid pressure. Surface displacement was tracked manually along the tank sidewall. I attempted to use similar solids concentrations and slurry depths in each replicate experiment; however, some variation occurred among experiments (Table 2).

The value of the diffusion coefficient,  $D$ , was estimated by minimizing the difference between predicted excess fluid pressure (Eqs 10, A1.1), for an assumed value of  $D$ , and measured pressure. For each experiment, differences between predicted and measured excess fluid pressure at several time steps were squared and summed. The square root of the summed-squares value was minimized to obtain a best-fit approximation of the diffusion coefficient. Similar minimization methods have been used to estimate parameter values in other applications of diffusion models (e.g., Rosenbloom and Anderson 1994).

## RESULTS

### Tank Experiments

**Initial Fluid Pressures.**—Measured initial fluid pressures were linear with depth (Fig. 4). Sediment composition and substrate boundary condition had negligible effect on the initial fluid-pressure profile (Fig. 4). Therefore, the physical mechanism that induces excess fluid pressure in consolidating slurries is independent of sediment composition, grain size, grain shape, or substrate influence.

Initial fluid pressures were approximately twice the local hydrostatic fluid pressures (Fig. 5; Table 2). Therefore, initial *excess* fluid pressures were of magnitude comparable to hydrostatic fluid pressures (cf. Eq 6). The measured fluid pressures strongly suggest that the slurries were liquefied immediately after they were poured into the tank (cf. Eqs 3–6), if the mixtures had typical porosities of 25 to 50 percent (e.g., Major et al. 1997). I have assumed that the slurries were indeed liquefied, and have estimated initial values of porosity ( $\phi$ ) at various depths (Table 2). Initial sediment concentrations ( $1 - \phi$ ) calculated from estimates of porosity compare favorably with measured concentrations of samples (Table 2), which further supports the notion that the experimental slurries were liquefied. Therefore, intergranular contacts initially bore little, if any, load even though more than 50 percent of the volume of each slurry was composed of solid particles.

**Transient Response of Total Fluid Pressure.**—Pore-fluid pressures nearly sufficient to cause liquefaction were sustained for a few tens of seconds to several hundreds of minutes among experiments (Fig. 5A–C). After grain contacts became well established and significant intergranular stresses developed, fluid pressure dropped rapidly. In experiment C4 (Fig. 5A), however, fluid pressure rose suddenly after about 50 minutes. This abrupt fluid-pressure increase at all levels in the slurry probably resulted from shifting of unstably packed grains. Pierson (1981) observed a similarly abrupt fluid-pressure increase when he inadvertently disturbed a static sediment slurry.

The character of the basal boundary significantly affected the response of basal fluid pressure but had limited effect on the pressure response at higher levels in the slurry. Pore-fluid seepage across the basal boundary enhanced dissipation of basal fluid pressure (Fig. 5). In experiments using loamy gravel, basal fluid pressure of nearly liquefaction magnitude persisted for no more than a few seconds to a few tens of seconds (Fig. 5A). In experiments using the clay-rich Osceola Mudflow debris (Fig. 5B), it persisted for several minutes to several tens of minutes, whereas at shallower depths it persisted for more than a day. In contrast, high basal fluid pressure persisted orders of magnitude longer when the bed was impermeable (Fig. 5).

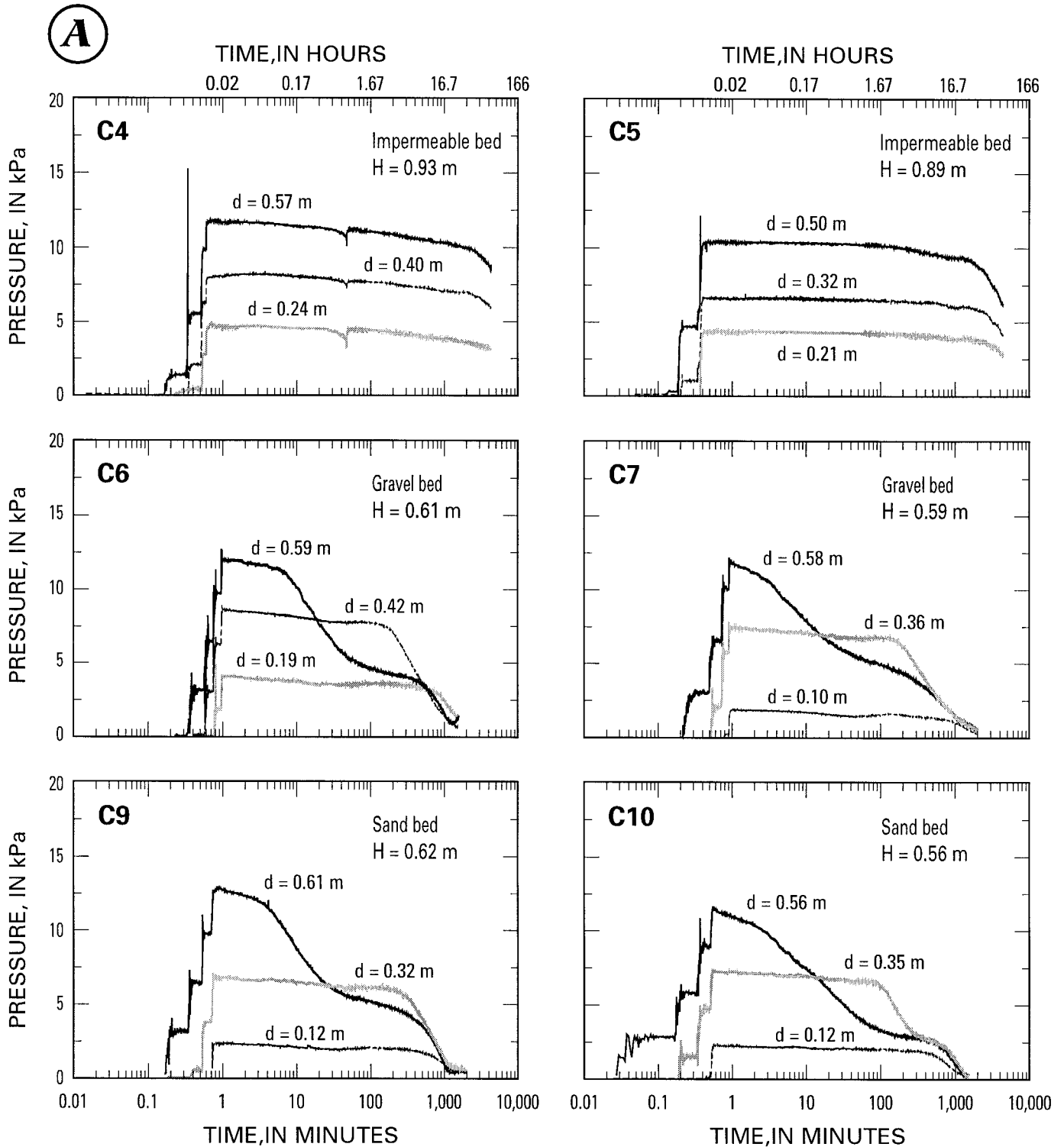


FIG. 5.—Total fluid pressure measured in one-dimensional tank consolidation experiments. Experimental debris includes: A) loamy gravel used at USGS debris-flow flume (see Table 1; deposit 052694); B) Osceola Mudflow from Mount Rainier; and C) Mount St. Helens 1980 North Fork Toutle River debris flow.  $H$  is the initial thickness of the slurry, and  $d$  represents the depth of the pressure probe below the surface of the slurry. Permeable gravel or sand basal boundaries are identified. Progressive abrupt peaks in the pressure signal result from discrete slugs of slurry poured into the consolidation tank. The initial fluid pressure is that value measured immediately after all of the slurry was poured into the tank. The hydrostatic pore-fluid pressure (in kilopascals) at each probe is approximately 10 times the depth of the probe.

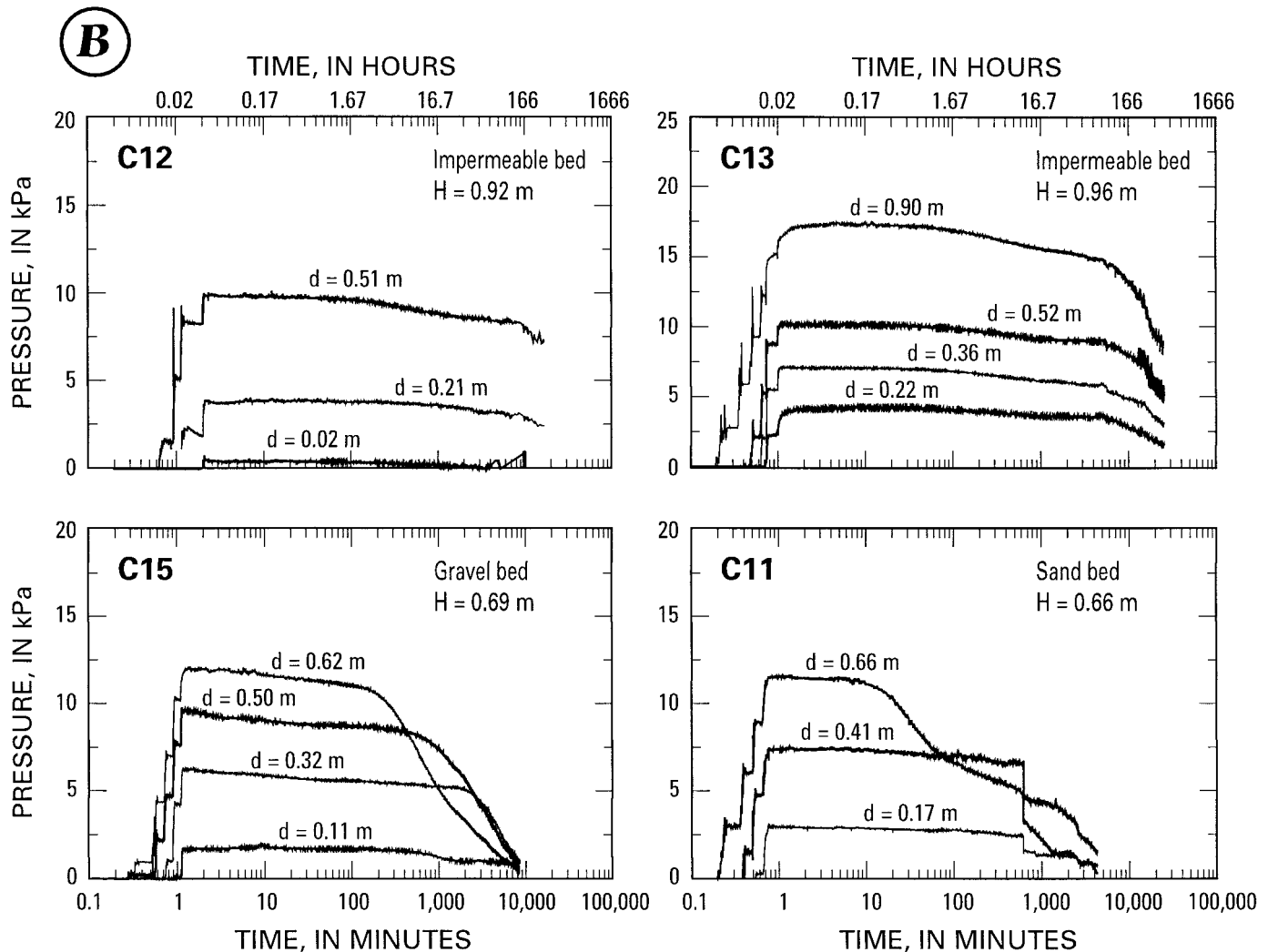


FIG. 5.—Continued.

**Diffusion of Excess Fluid Pressure.**—The model of gravity-driven consolidation predicts that dissipation of excess fluid pressure begins at the *base* and advances upward through a slurry (Fig. 6). This response contrasts markedly with that predicted by analyses that neglect body forces, in which pressure dissipation begins at a drainage surface and migrates inward (e.g., Lambe and Whitman 1969). The response predicted by the self-consolidation model is a direct consequence of the initial-pressure condition caused by undrained gravitational loading. When the basal boundary is impermeable, the greatest excess fluid pressure occurs at the base of the slurry (Figs. 4, 6) and establishes a pressure gradient that drives flow upward. When the basal boundary drains freely, the distribution of excess fluid pressure is nonsymmetrical and the locus of maximum excess fluid pressure is displaced upward from the bed (Fig. 6). However, the greatest excess fluid pressure remains in the lower part of the slurry, which drives the advancing dissipation front upward.

The magnitude of substrate permeability had little effect on the evolving fluid-pressure field in the experimental slurries. Substrate permeabilities exceeded slurry permeabilities (Table 1) by a factor of 10 or more. The gravel and sand beds had mean permeabilities of  $3 \times 10^{-10} \text{ m}^2$  and  $7 \times 10^{-11} \text{ m}^2$ , respectively (Major 1996). Despite order-of-magnitude variation in substrate permeability, predicted and measured responses of excess fluid pressure are similar for both the gravel and sand substrates (Fig. 6).

Estimated slurry diffusivities locally ranged from about  $10^{-5}$  to  $10^{-9} \text{ m}^2/\text{s}$  (Table 3). In general, however, the estimated diffusivities fell in a remarkably narrow range,  $10^{-6}$  to  $10^{-7} \text{ m}^2/\text{s}$ , given the spectrum of slurry compositions. These estimated diffusivities are probably reasonable to better than an order of magnitude. Values of  $D$  shown in Figure 6 provide the best overall correspondence between predicted

and measured excess pore-fluid pressure across the depth of the slurry. These values generally coincide with estimates based on change in fluid pressure measured at an intermediate-depth probe.

In nearly all experiments the diffusivity decreases with slurry depth, in rare cases by a few orders of magnitude (Table 3). Depthwise variation of  $D$  appears to be most pronounced in the permeable-bed experiments, but that appearance may reflect a lack of near-base data in the impermeable-bed experiments. Depth dependence of  $D$  indicates depth-dependent structure in grain packing, and suggests that gravitational consolidation of shallow slurries subjected to low effective stresses is a non-linear process that is stress-field dependent.

**Effective Stress.**—As excess pore-fluid pressure decays during gravitational consolidation, effective stress also evolves upward (Fig. 7). Prediction of effective stress requires an estimate of  $D$  as well as an estimate of slurry porosity  $\phi$  (cf. Eq 11). The evolving stress profiles illustrated in Figure 7 incorporate optimal diffusivity coefficients (Fig. 6; Table 3) and mean initial porosities (Table 2) for each slurry. Effective stress converges toward a linear profile as excess fluid pressure dissipates. The linear profile represents the difference between the total stress and a hydrostatic fluid pressure (cf. Fig. 2C). Soil mechanics refer to this state (zero excess fluid pressure) as the drained condition (e.g., Craig 1992). Given sufficient time, deposit water would drain completely and effective stress would converge to a total-stress profile for dry sediment.

Basal drainage permits rapid development of significant effective stress near the bed. At a permeable boundary, excess fluid pressure dissipates instantly and effective stress achieves its maximum value (Fig. 7B). Sharp curvature of the stress profile during early stages of consolidation, however, shows that a slurry overlying a

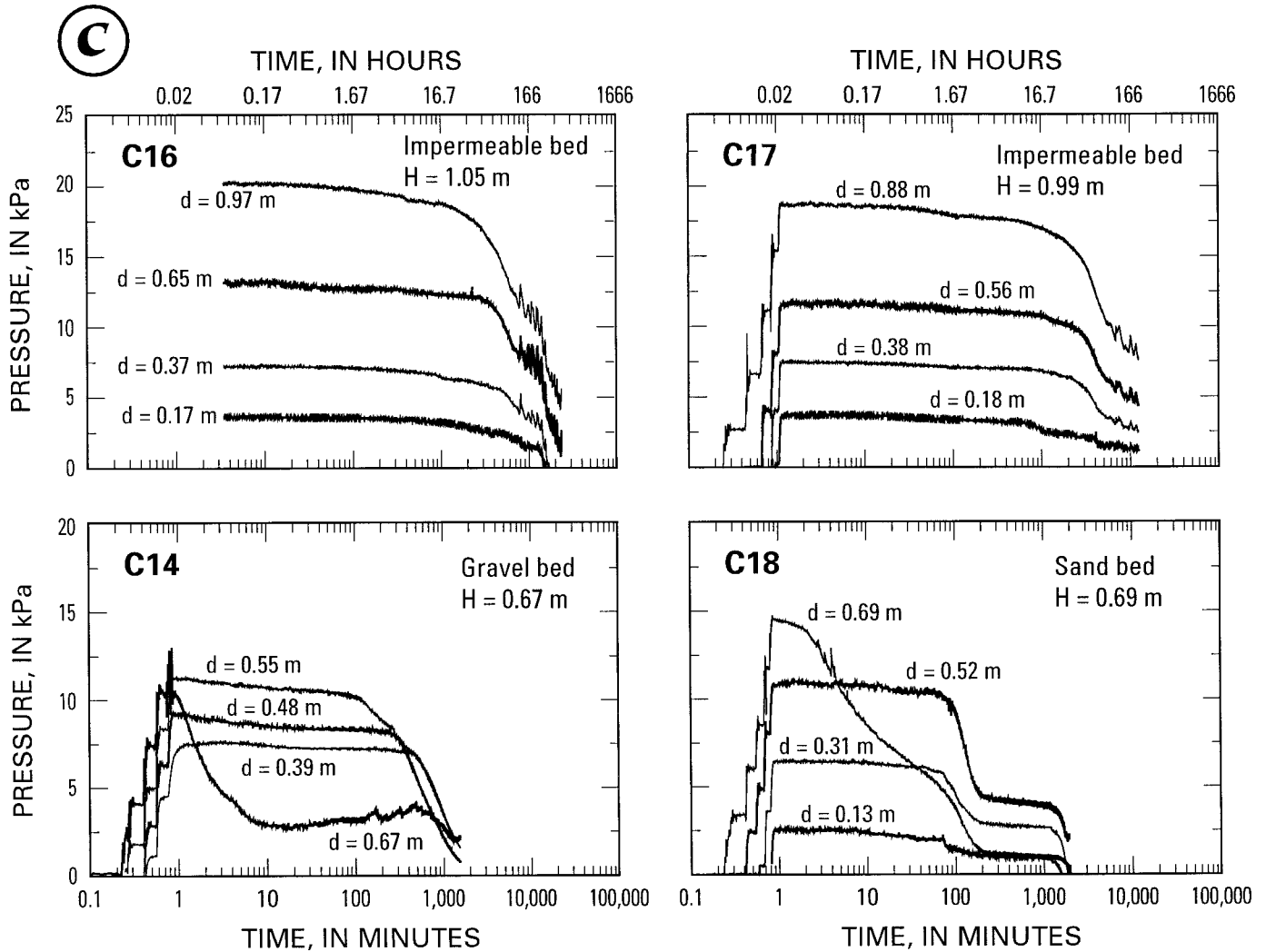


FIG. 5.—Continued.

drained boundary develops a substantial stress gradient in its lower stratum. Even though the basal boundary is drained, a substantial body of liquefied to nearly liquefied debris can overlie a relatively narrow band of frictionally “locked” debris. In the example shown (Fig. 7B), effective stress at a depth 85% below the slurry surface (i.e.,  $z/H = 0.15$ ) is 25% of the maximum basal effective stress at nondimensional time  $T_* = 0.03$  (cf. Fig. 6), whereas at a depth 95% below the surface the effective stress is 70% of the maximum basal effective stress. As excess fluid pressure dissipates, the sharp stress gradient relaxes. In contrast, effective stress evolves more slowly along an impermeable bed (Fig. 7A), and substantial stress gradients do not develop. In this case a thin band of frictionally “locked” debris does not develop at the bed.

**Surface Displacement.**—Displacements of slurry surfaces ranged from a few centimeters to several centimeters. Compared to original slurry depth, these displacements were relatively small. Minimum estimates of bulk volume strain, averaged over an entire stratum, ranged from 3 to 10 percent (Major 1996); average bulk volume strain was about 5 percent.

Prediction of surface displacement requires an estimate of the effective compressibility of debris (cf. Eq. 12). It is difficult, however, to generalize the compressibility of slurries. Reported compressibilities of clay-rich slurries range from  $10^{-5}$  to  $10$   $\text{kPa}^{-1}$  (Carrier et al. 1983); there are few if any compressibilities reported for sand-dominated slurries. It is inappropriate to use estimates of compressibility reported for sandy soils (e.g., Lambe and Whitman 1969) for two reasons: (1) values of elastic moduli are highly sensitive to experimental conditions, especially at low effective stresses (e.g., Hicher 1996), and (2) physical properties of sand-dominated

slurries can differ significantly from those of compacted sands tested by traditional geotechnical methods (Major et al. 1997). Rather than use questionable estimates of compressibility, I compared surface displacements predicted using a range of compressibilities (reciprocal of constrained modulus,  $E_c$ ) with measured surface displacement. Matching predicted displacement profiles to measured displacements indicates that effective compressibilities of these slurries were about  $0.01$   $\text{kPa}^{-1}$  ( $E_c = 50$ – $100$   $\text{kPa}$ ) (Fig. 8).

#### Debris-Flow-Flume Deposits

Transient response of excess fluid pressure at the base of debris-flow-flume deposits (cf. Major 1997; Major and Iverson 1999) is similar to that documented for the impermeable-bed tank experiments (Fig. 9). However, there are two primary differences. (1) The flume deposits were thin (as little as 10% of the tank-slurry thicknesses); hence, excess fluid pressure in the flume deposits dissipated more rapidly. (2) Reported diffusivities for the flume deposits represent optimal fits between predicted pressure profiles and measured basal excess pore-fluid pressures (cf. Fig. 1). As discussed above, diffusivity generally is least at the base of gravitationally consolidating debris and thus may not be representative of the debris mass. Hydraulic diffusivities of the flume deposits therefore represent minimum estimates.

Measurements of transient basal fluid pressure in the flume deposits demonstrates that modest amounts of fine sediment, and possibly permeability heterogeneity, can significantly influence pore-fluid hydraulics in consolidating debris-flow deposits. Deposits composed of sandy gravel that contained  $<2\%$  mud had characteristic

TABLE 3.—Values of optimal diffusivity coefficient

Experiment*	Basal Boundary†	Slurry Depth $H$ (m)	Domain Level $z$ (m)	$D$ (m <sup>2</sup> /s)	Optimal $D$ (m <sup>2</sup> /s)	$C_{1\ddagger}$ (m <sup>2</sup> /s)
C4	I	0.93	0.69	$3.0 \times 10^{-6}$	$1.6 \times 10^{-6}$	
			0.54	$1.6 \times 10^{-6}$		
			0.37	$1.3 \times 10^{-6}$		
C5	I	0.89	0.68	$1.3 \times 10^{-6}$	$1.3 \times 10^{-6}$	
			0.57	$1.3 \times 10^{-6}$		
			0.39	$1.3 \times 10^{-6}$		
C6	P	0.61	0.42	$9 \times 10^{-7}$	$1.3 \times 10^{-6}$	
			0.20	$1.3 \times 10^{-6}$		
			0.03	$9 \times 10^{-7}$		
C7	P	0.59	0.49	$5 \times 10^{-6}$	$1.4 \times 10^{-6}$	
			0.23	$1.4 \times 10^{-6}$		
			0.01	$3.1 \times 10^{-7}$		
C8	P	0.58	0.45	$4.3 \times 10^{-6}$	$1.2 \times 10^{-6}$	
			0.25	$1.2 \times 10^{-6}$		
			0.00	$9.5 \times 10^{-9}$		
C9	P	0.62	0.50	$4.6 \times 10^{-6}$	$2.3 \times 10^{-6}$	
			0.29	$2.3 \times 10^{-6}$		
			0.01	$1.6 \times 10^{-7}$		
C10	P	0.56	0.45	$3.4 \times 10^{-6}$	$2.8 \times 10^{-6}$	$1.4 \times 10^{-6}$
			0.22	$2.8 \times 10^{-6}$		
			0.00	$4.6 \times 10^{-8}$		
C11	P	0.66	0.49	$4.2 \times 10^{-6}$	$1.5 \times 10^{-6}$	$1.2 \times 10^{-6}$
			0.25	$1.5 \times 10^{-6}$		
			0.02	$1.2 \times 10^{-7}$		
C12	I	0.91	0.90	$1.5 \times 10^{-5}$	$3.3 \times 10^{-7}$	$8.6 \times 10^{-7}$
			0.70	$6.5 \times 10^{-6}$		
			0.40	$3.3 \times 10^{-7}$		
C13	I	0.96	0.74	$6.2 \times 10^{-7}$	$4.9 \times 10^{-7}$	$5.4 \times 10^{-7}$
			0.60	$5.8 \times 10^{-7}$		
			0.44	$4.0 \times 10^{-7}$		
C14	P	0.67	0.28	$1.3 \times 10^{-6}$	$4.8 \times 10^{-7}$	$1.6 \times 10^{-6}$
			0.19	$5.3 \times 10^{-7}$		
			0.12	$4.8 \times 10^{-7}$		
C15	P	0.69	0.00	$1.3 \times 10^{-7}$	$4.0 \times 10^{-7}$	$5.4 \times 10^{-7}$
			0.58	$6.0 \times 10^{-6}$		
			0.37	$3.8 \times 10^{-7}$		
C16	I	1.05	0.19	$4.3 \times 10^{-7}$	$1.0 \times 10^{-6}$	$8.6 \times 10^{-7}$
			0.07	$1.4 \times 10^{-7}$		
			0.88	$2.5 \times 10^{-6}$		
C17	I	0.99	0.68	$2.5 \times 10^{-6}$	$1.9 \times 10^{-6}$	$2.5 \times 10^{-6}$
			0.40	$1.2 \times 10^{-6}$		
			0.08	$9.0 \times 10^{-7}$		
C18	P	0.69	0.80	$7.0 \times 10^{-6}$	$5.5 \times 10^{-6}$	$2.6 \times 10^{-6}$
			0.60	$2.3 \times 10^{-6}$		
			0.43	$1.6 \times 10^{-6}$		
			0.10	$1.2 \times 10^{-6}$		
			0.56	$5.2 \times 10^{-5}$		
			0.39	$1.0 \times 10^{-5}$		
			0.18	$3.3 \times 10^{-6}$		
			0.01	$1.5 \times 10^{-7}$		

\* See Table 2 for material composition.

† I = impermeable basal boundary; P = freely draining permeable boundary.

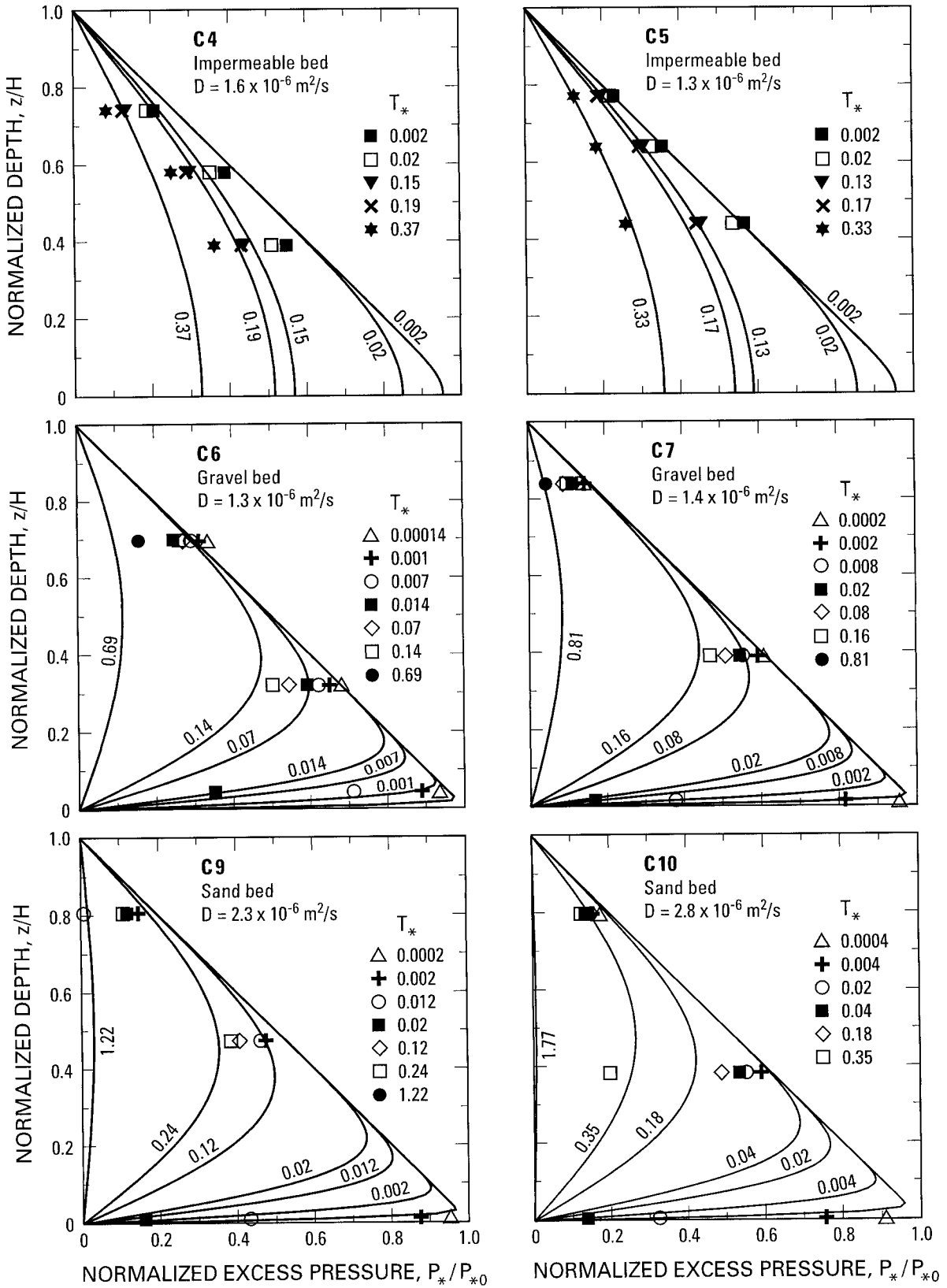
‡ Consolidation coefficient determined by (t)<sup>2</sup> method (ASTM 1995). This coefficient, identical in definition to  $D$ , but estimated from changes in surface displacement instead of fluid pressure, is a standard parameter in soil mechanics evaluations of consolidation.

diffusivities of order  $10^{-2}$  to  $10^{-4}$  m<sup>2</sup>/s (e.g., Fig. 9A, B; Table 1). Those composed of loamy gravel that contained about 2–4% mud, however, had characteristic diffusivities of order  $10^{-6}$  to  $10^{-7}$  m<sup>2</sup>/s (e.g., Fig. 9C, D; Table 1). Estimated diffusivities of the loamy-gravel deposits are comparable to values estimated from tank experiments using similar debris (Table 3). The large diffusivities ( $10^{-2}$  m<sup>2</sup>/s) estimated for two sandy-gravel deposits (not shown) may have been influenced by experimental conditions. In those experiments, flows were deliberately impeded by a wall located immediately downslope from the instrumentation plate (Iverson et al.

1994). Vigorous interaction between the flows and the wall resulted in chaotic, wedge-shaped deposits having their thickest ends braced against the wall. Unlike experiments in the smooth-walled tank, there was significant friction between those flume deposits and the wooden wallboard. Strikingly rapid dissipation of fluid pressure in those two deposits suggests that particle bridging, frictional drag at the wall, and perhaps development of high-permeability flowpaths affected the fluid-pressure response. Therefore, those diffusivities may not properly represent hydraulic properties of sandy-gravel deposits.

Fig. 6.—Comparison of predicted and measured evolution of excess pore-fluid pressure across slurry depth in experiments on gravity-driven consolidation. Predicted pressure profiles (solid lines) are based on an optimal value of the diffusivity coefficient,  $D$ , that minimizes the difference between predicted and measured values of excess fluid pressure (see text). Excess pore-fluid pressure ( $P_*$ ) is normalized by the initial value of excess pore-fluid pressure at the base of the slurry ( $P_{*0}$ ). Position within the slurry ( $z$ ) is normalized by slurry depth ( $H$ ). Position along the pressure profile represents predicted excess fluid pressure as some fraction of the initial basal excess fluid pressure. Each curve represents a different increment in time. Symbols represent fluid pressure measured at corresponding times. Time is normalized to remove effects of depth variations among experiments. Nondimensional time ( $T_*$ ) is represented by  $t/[(H^2/D)]$  in the impermeable-bed experiments and by  $t/[(H/2)^2/D]$  in permeable-bed experiments. Experimental debris includes: **A**) loamy gravel used at the USGS debris-flow flume (see Table 1; deposit 052694); **B**) Osceola Mudflow from Mount Rainier; and **C**) Mount St. Helens 1980 North Fork Toutle River debris flow. Permeable-bed and impermeable-bed experiments are identified.

**A**



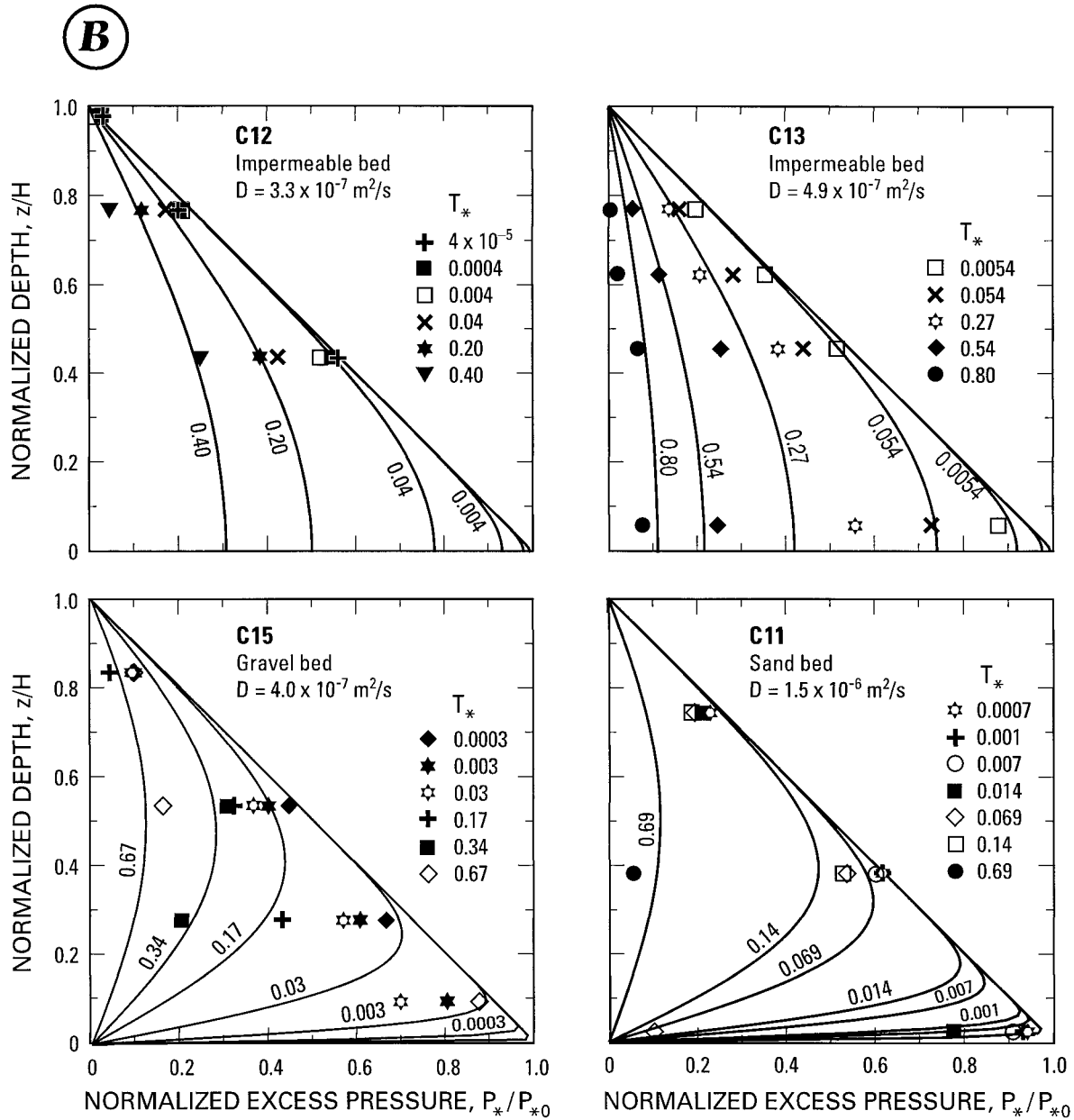


FIG. 6.—Continued.

## DISCUSSION

A linear consolidation model, valid strictly for infinitesimal strain, reasonably describes self-weight consolidation of noncohesive sandy slurries despite measured volume changes as large as several percent and data that suggest that hydraulic diffusivities may be stress-field dependent. The general timing of consolidation is satisfactorily predicted if diffusivities of debris containing at least a few percent mud are of order  $10^{-6}$  to  $10^{-7}$   $\text{m}^2/\text{s}$ . Magnitudes of consolidation settlement are described well if the slurries are highly compressible ( $C \sim 0.01 \text{ kPa}^{-1}$ ). Optimal diffusivities estimated for the experimental slurries are several orders of magnitude smaller than values common for most well-sorted, unlithified granular sediment, but are comparable to values reported for tills (e.g., Roeloffs 1996).

We gain insight regarding the low diffusivity values, and perhaps into apparent consolidation nonlinearity, by considering the physical parameters that affect diffusivity. Diffusivity is inversely proportional to fluid viscosity. Thus, deviation of fluid viscosity from that of clear water can reduce hydraulic diffusivity. In debris that contains abundant colloidal clay, or clay that is highly reactive to water, fluid

viscosity (and fluid strength) can greatly affect pore-fluid hydraulics (e.g., Martosudarmo and Johnson 1997). Even in the absence of colloids, noncohesive sediment can alter fluid viscosity (Einstein 1906; Poletto and Joseph 1995). Effluent collected from flume deposits was composed of sediment and water; silt and clay sizes dominated sediment composition, and volumetric concentrations were typically a few percent (Major 1996). Only clear fluid was expelled during tranquil consolidation of tank slurries. Low sediment concentrations of both flume-deposit and tank-deposit effluents suggest that pore-fluid viscosity differed from that of clear water by less than about 70% (Major 1996). Thus high fluid viscosity does not explain the estimated diffusivity magnitudes.

Changes in permeability and effective compressibility of slurries during consolidation are more important than altered fluid viscosity. Diffusivity is directly proportional to permeability, but inversely proportional to compressibility, of the granular matrix. As excess fluid pressure dissipates, grains pack closer together, which reduces porosity. As a result, the mixture becomes harder to compress owing to the stiffness imparted by increasingly robust intergranular contacts. Therefore, both permeability and effective compressibility decrease as packing density increases. If

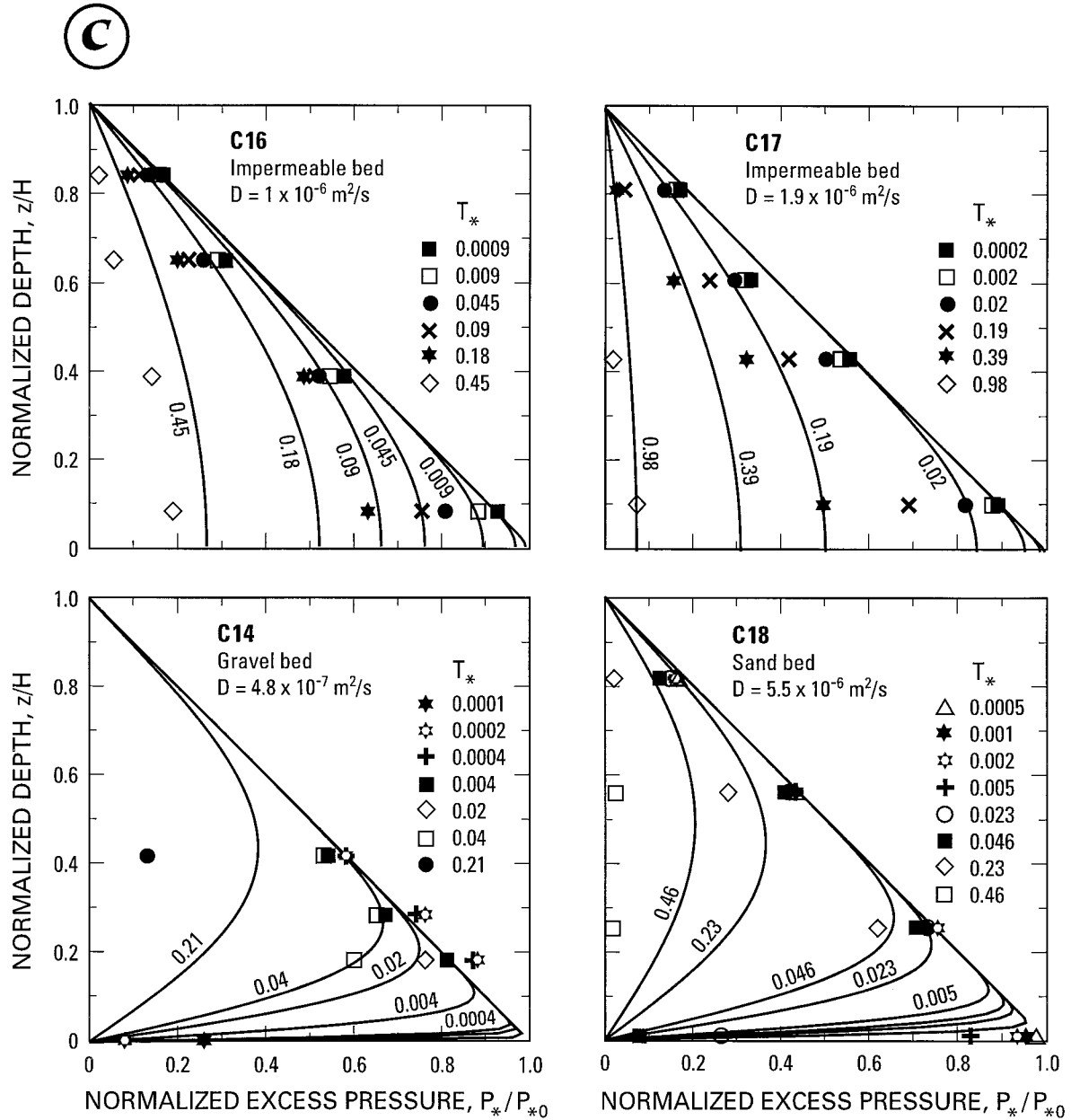


FIG. 6.—Continued.

changes in these physical properties of consolidating debris are of approximately equal magnitude, then diffusivity of the debris remains nearly constant. If changes in permeability are more important than changes in compressibility, then the hydraulic diffusivity should decrease as packing density changes. On the other hand, if the increased stiffness of intergranular contacts is more important than changes in permeability, then the hydraulic diffusivity should increase with time as excess fluid pressure dissipates, and the rate of pressure dissipation should accelerate. This is not the trend observed in the experiments. Instead, the experiments suggest that diffusivity decreases as porosity decreases. Observed discrepancies between predicted and measured dissipation of excess fluid pressure indicate that changes in permeability more than compensate for changes in compressibility, and impart greater influence on apparent consolidation nonlinearity.

Influence of mixture permeability and compressibility on consolidation nonlinearity can be assessed further by considering their relationships to effective stress (Iverson 1997a). Porosity of sediment mixtures commonly declines logarithmically as effective stress increases (e.g., Lambe and Whitman 1969; Been and Sills 1981; Major et al. 1997), and permeability of debris-flow mixtures varies exponentially

with porosity (e.g., Major et al. 1997). As a result, changes in porosity of as little as a few percent can cause more than ten-fold changes in permeability (Major 1996; Major et al. 1997). Iverson (1997a) postulated that compressibility of debris-flow mixtures varies inversely with effective stress,  $C \approx \kappa/\sigma_e$ , where  $\kappa$  is a positive proportionality coefficient, combined this postulate with relationships among permeability, porosity, and effective stress, and showed that

$$D = \frac{k_0 e^{a\phi_*}}{\mu \kappa} \sigma_e^{1-a\kappa} \sigma_*^{a\kappa} \quad (13)$$

In this expression  $k_0$ ,  $\phi_*$ , and  $\sigma_*$  represent characteristic values of permeability, porosity, and effective stress, respectively, and  $a$  is a coefficient that characterizes the dependence of permeability on porosity. When  $a\kappa > 1$ , diffusivity decreases as effective stress increases because changes in permeability more than compensate for changes in compressibility. In contrast, when  $a\kappa < 1$ , diffusivity increases as effective stress increases because changes in compressibility outweigh changes in permeability. When  $a\kappa$  is close to 1, diffusivity depends weakly on effective stress and

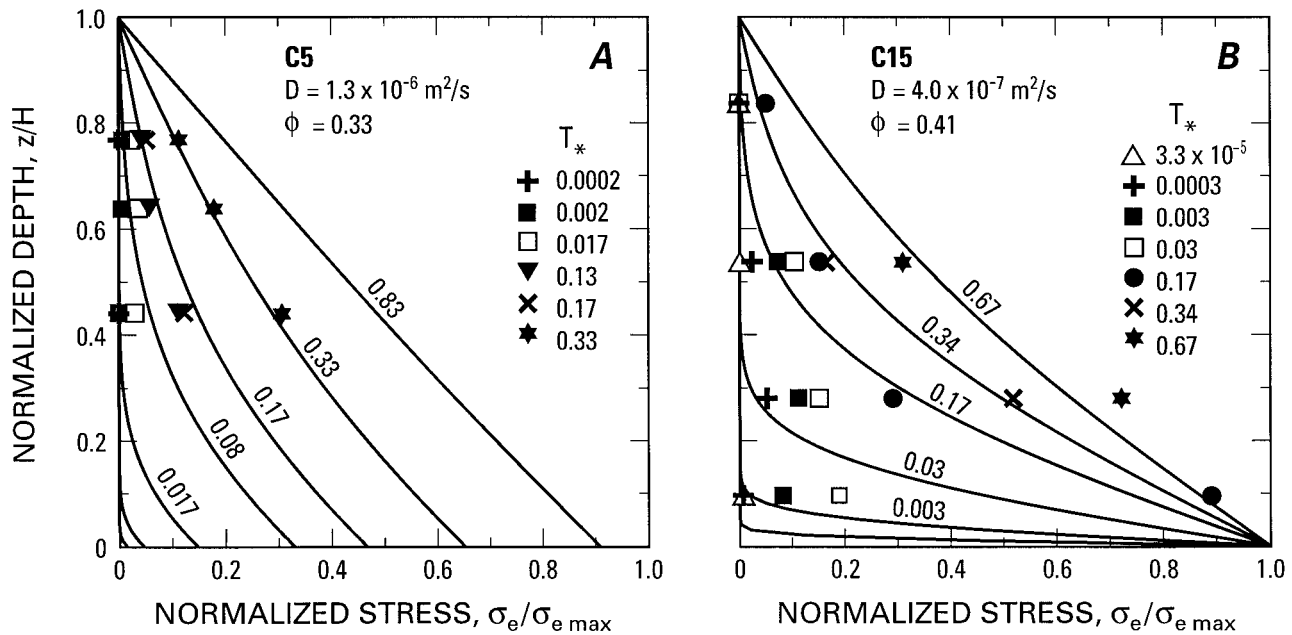


Fig. 7.—Representative examples of evolution of effective stress in experiments on gravity-driven consolidation. The effective stress has been normalized by the maximum basal effective stress. Position along stress profiles represents predicted effective stress as some fraction of the maximum basal effective stress. Each curve represents a different increment in time. Symbols represent effective stress measured at corresponding times. Time is normalized (see Figure 6). A) Impermeable-bed experiment using loamy gravel (see Figure 6A). B) Permeable-bed experiment using Osceola Mudflow debris (see Figure 6B).  $\phi$  is the mean value of initial porosity (see Table 2).

a constant diffusivity reasonably describes consolidation behavior (Iverson 1997a). Values of  $a$  are obtained from experimental relations between permeability and porosity. For several debris-flow mixtures,  $a \approx 10\text{--}30$  (Major et al. 1997). Values of  $\kappa$  are obtained from experimental relations between porosity and effective stress. Limited data for mud suspensions and debris-flow mixtures suggest that  $0.02 < \kappa \leq 0.05$  (e.g., Been and Sills 1981; Major 1996; Iverson 1997a; Major et al. 1997). These values suggest that  $a\kappa$  varies around a value of 1. When debris-flow mixtures are highly diluted, the product attains values  $>1$ ; less diluted mixtures attain values  $\leq 1$ . This subtle dependence of diffusivity on effective stress explains why consolidation of some experimental slurries is described well by a linear model, and others less so.

Permeabilities of sediment used in these experiments are not extraordinarily low for poorly sorted sandy debris. Permeabilities of compacted specimens varied from  $10^{-9}$  to  $10^{-14} \text{ m}^2$  (Major et al. 1997), and permeabilities of slurried sediment were of order  $10^{-12}$  to  $10^{-13} \text{ m}^2$ . Therefore, permeability alone cannot account for low diffusivity. Instead, the magnitude of diffusivity appears to be influenced strongly by slurry compressibility. Measured surface displacements indicate that slurry compressibilities are about  $10^{-2} \text{ kPa}^{-1}$ . This is about 1000 times greater than that of typical sandy soil (Lambe and Whitman 1969; Major et al. 1997). Diffusivity is inversely proportional to compressibility; thus, the large compressibility of diluted debris-flow mixtures under low effective stresses is a key factor contributing to their low diffusivity. Effectively low diffusivities and their influence on pore-fluid pressure contribute vitally to debris-flow mobility (Iverson 1997a) as well as to post-depositional consolidation.

Consolidation of debris flow deposits is affected by boundary conditions as well as by contemporaneous changes in the physical structure of the deposit. A permeable substrate permits more rapid changes in fluid pressure and effective stress than does an impermeable substrate by providing an additional pathway for fluid migration. The effect of substrate permeability is illustrated clearly in Figures 5–7. The magnitude of substrate permeability, however, does not affect the transient field responses as long as the substrate is distinctly more permeable than the slurry; fluid migration is controlled by properties of the deposit, not of the substrate. If the permeability of the substrate approaches that of the deposit, it may act effectively as an impermeable boundary.

Even if a substrate provides an additional pathway for fluid migration, structural changes at the base of a deposit may inhibit fluid loss. Changes in packing at the base of a deposit reduce porosity and permeability and hinder subsequent escape of fluid. Fluid loss at the base of a deposit therefore triggers a sort of “self-sealing” that retards basal fluid migration. As a result, excess fluid pressure slightly above

the bed may not dissipate as rapidly as predicted by a linear consolidation model, even in the presence of a high fluid-pressure gradient (Fig. 6; e.g., experiments C11, C15).

Transient behavior of fluid pressure and effective stress in consolidating debris limits several hypotheses for debris-flow deposition. Infiltration loss has been suggested as a mechanism to explain debris-flow deposition (e.g., Jahns 1949; Hooke 1967, 1987; Brococo and Thomson 1969; Costa 1984), but my results suggest that changes in grain fabric retard fluid loss and pressure dissipation near the base of a slurry. Thus, infiltration loss may have only limited influence on debris-flow deposition. This inference is bolstered by field measurements of fluid loss obtained by Okuda et al. (1981). They placed groundwater sensors along the paths of debris flows on an alluvial fan and found that water did not infiltrate vertically into the substrate while flows were in transit. My results furthermore show that consolidation progress migrates upward from the base of the debris. Therefore, if homogeneous debris flows consolidate during transit, as proposed by Terzaghi (1956) and Hutchinson (1986), frictional forces resisting motion first exceed forces driving motion at the base of a flow. If so, a depositional front should migrate upward through a flow. Experiments with dry glass beads flowing down a chute (Vallance 1994) show that depositional fronts can migrate upward in some mass flows. This style of deposition, however, departs markedly from that depicted by the popular Bingham viscoplastic model for debris flows, in which sediment is deposited abruptly *en masse* when an intrinsic yield strength of debris exceeds driving forces (Johnson 1970). Significant consolidation of debris flows does not occur during transit, however. Iverson (1997a) measured liquefaction fluid pressures behind flow fronts in large experimental debris flows, and Major and Iverson (1999) showed that those fluid pressures persist through deposition. If flows consolidated significantly during transit, measured fluid pressure would be well below liquefaction level. Collectively, the following observations and measurements led Iverson (1997a) and Major and Iverson (1999) to the inescapable conclusion that debris-flow deposition results primarily from intergranular friction and bed friction concentrated at flow margins rather than from widespread dissipation of excess pore-fluid pressure or from a uniform viscoplastic yield strength: (1) the unimportance of infiltration loss at the bed, (2) liquefaction fluid pressure measured in debris-flow interiors during transit and deposition, (3) a lack of high pore-fluid pressure at flow margins during transit and deposition, and (4) restriction of significant fluid-pressure dissipation to post-depositional consolidation.

Analysis of gravity-driven consolidation provides insight into the geomorphic and sedimentologic character of debris-flow deposits. Remobilization and erosion of antecedent debris is governed by the ability of subsequent flow to overcome resisting stresses in a deposit (e.g., Mohrig et al. 1999). If resisting stresses in a deposit are

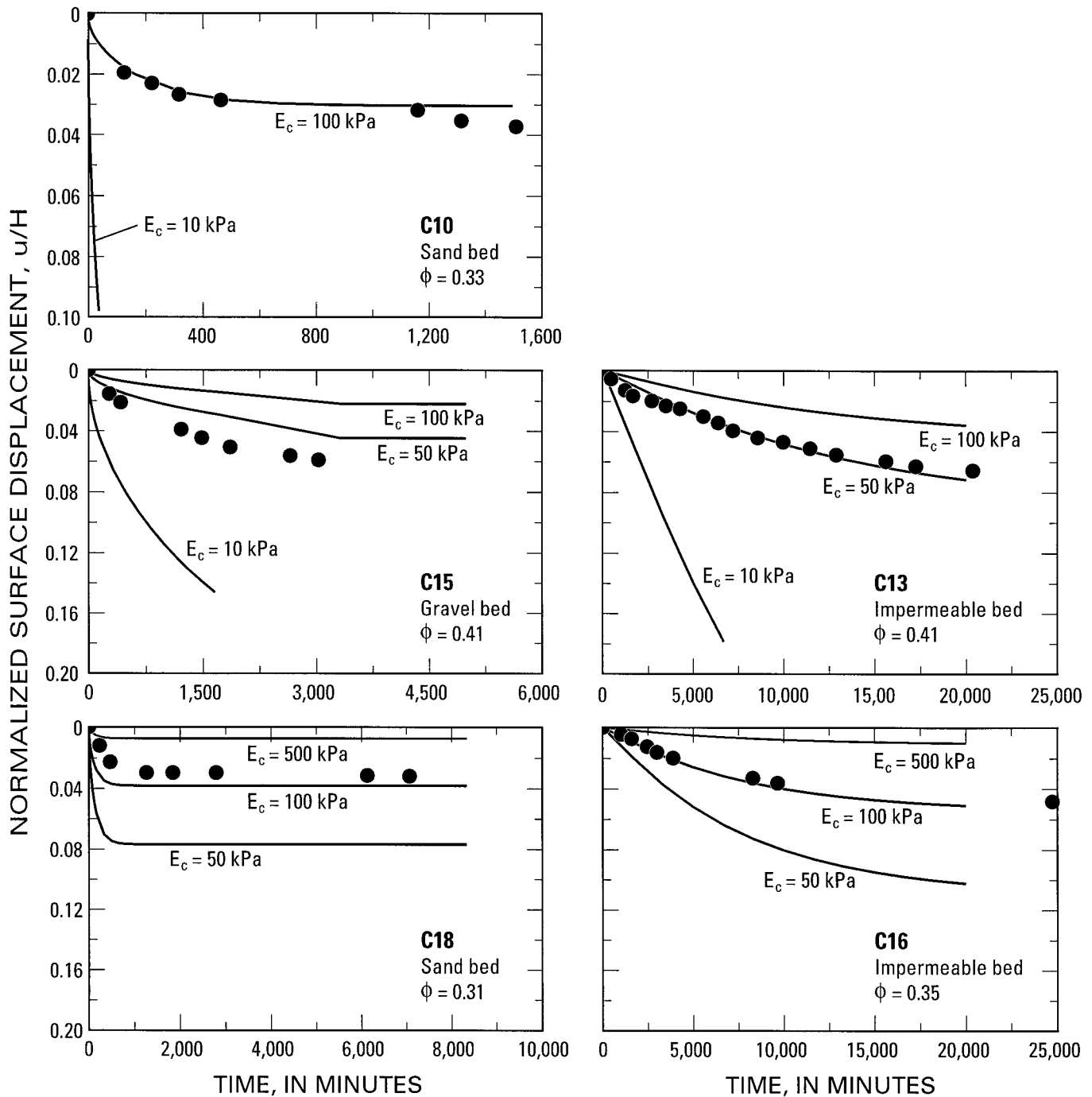


FIG. 8.—Comparison of predicted (solid lines) and measured (symbols) evolution of surface displacement in experiments on gravity-driven consolidation. Surface displacement ( $u$ ) is normalized by initial slurry depth. Predicted profiles (using optimal value of  $D$ ; Fig. 6) for various values of constrained modulus are shown. See Figure 6 for slurry compositions.

low, even minor shear coupling with a subsequent flow may induce remobilization. Observed waves translating through, or across and enveloping, freshly deposited debris (e.g., Sharp and Nobles 1953; Morton and Campbell 1974; Wasson 1978; Costa and Williams 1984) attest to the ability of debris flows to remobilize deposits. These observations are difficult to reconcile with a Bingham viscoplastic material. If deposition is related to an intrinsic uniform yield strength of debris, then for a deposit to remobilize, its yield strength must be exceeded. However, application of a stress in excess of the yield strength requires remobilization of the full thickness of a deposit, and not just its upper part. Analysis of gravity-driven consolidation shows that effective stresses

evolve upward from the base of a stratum; such a stress field can foster partial remobilization of deposits, because resisting stresses are not uniform through the stratum (cf. Fig. 7).

Many debris flows occur as a series of surge waves, with surge periods ranging from seconds to several minutes or more (e.g., Jahns 1949; Sharp and Nobles 1953; Morton and Campbell 1974; Wasson 1978; Costa and Williams 1984; Zhang 1993). Comparison of typical surge periods with characteristic times for dissipation of fluid pressure demonstrates that freshly deposited debris has the potential to be remobilized easily. The characteristic pressure-dissipation time is defined as  $L^2/D$ , where  $L$  is a

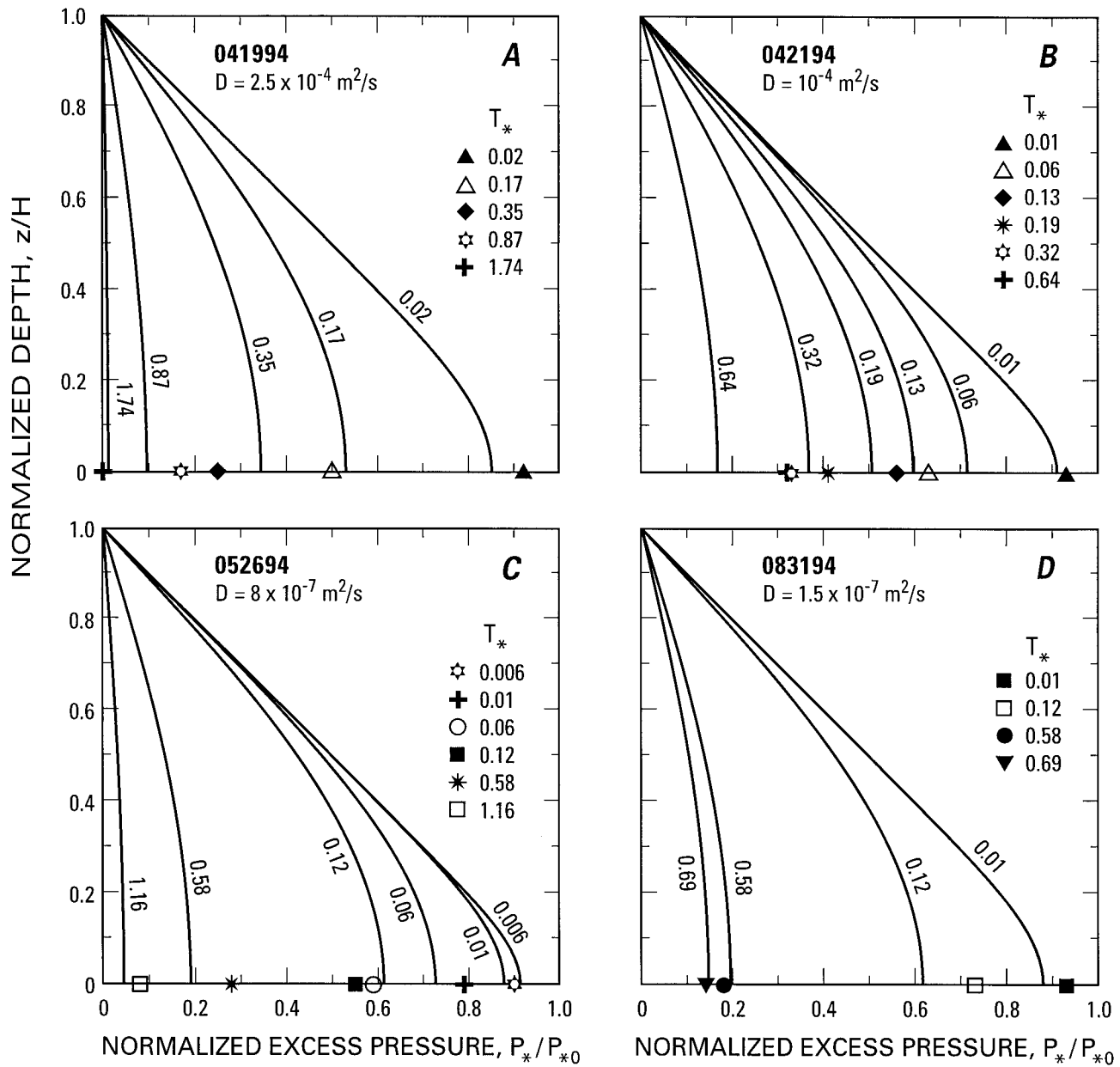


FIG. 9.—Comparison of predicted (for optimal value of  $D$ ) and measured evolution of excess pore-fluid pressure at base of representative experimental debris-flow deposits at USGS debris-flow flume. The excess pore-fluid pressure is normalized by the initial value of excess pore-fluid pressure. See Figure 1 and Table 1 for debris composition. Each curve represents an increment of time. Symbols represent fluid pressure measured at corresponding times. Time is normalized to remove variations in deposit thickness among experiments (see Figures 1 and 6).

characteristic length scale of fluid migration. For deposits overlying an impermeable bed,  $L$  is the thickness of the deposit,  $H$ . For deposits overlying a permeable bed,  $L = (1/2)H$ . Large ratios of surge period to pressure-dissipation time ( $\xi \gg 1$ ) indicate that excess fluid pressure dissipates rapidly relative to the surge period; thus, deposits are not easily remobilized. Small ratios ( $\xi \ll 1$ ) indicate that excess fluid pressure dissipates slowly relative to the surge period; thus, deposits have potential for easy remobilization. Table 4 shows values of  $\xi$  for hypothetical surge periods of several seconds (0.01 hours) to several (10) hours. Pressure-dissipation times were  $>10$  hours in all but 6 of 22 flume and tank deposits. Pressure-dissipation times fell between 0.01 and 10 hours in 5 of the remaining 6 deposits. These results indicate that most freshly deposited debris is probably remobilized by recurrent surging during a single debris flow, and also that it is probably remobilized at least locally during emplacement of multiple debris flows that may occur over hours, days, or weeks. Remobilization of

debris can obliterate stratigraphic distinction among multiple events and may cloud correct sedimentologic interpretation of depositional process (cf. Major 1997).

## CONCLUSIONS

Self-loading drives consolidation of debris-flow deposits. Excess pore-fluid pressure in debris-flow deposits results from a downward flux of buoyant sediment rather than from external surface loading. A linear, one-dimensional diffusion model satisfactorily approximates the overall timing and magnitude of postdepositional consolidation of noncohesive debris-flow slurries. Diffusivities of debris containing at least a few percent mud are of order  $10^{-6}$  to  $10^{-7} \text{ m}^2/\text{s}$ ; sandy-gravel deposits having less than 2 percent mud are characterized by larger diffusivities,  $10^{-4} \text{ m}^2/\text{s}$ . Mag-

TABLE 4.—Comparison of hypothetical surge periods (0.01 hours and 10 hours) to characteristic fluid-pressure dissipation times

Deposit Number	Optimal $D$ (m <sup>2</sup> /s)	$H$ (m)	$L$ (m)	$L^2/D$ (s)	$\xi$	
					0.01 hours	10 hours
041994	$2.5 \times 10^{-4}$	0.120	0.120	58	0.6	620
042194	$1 \times 10^{-4}$	0.125	0.125	156	0.2	230
052694	$8 \times 10^{-7}$	0.083	0.083	8611	<0.1	4
062194	$4 \times 10^{-2}$	0.420	0.420	4	10	9000
062394	$2 \times 10^{-3}$	0.330	0.330	54	0.7	670
072094	$8.5 \times 10^{-7}$	0.070	0.070	5765	<0.1	60
083194	$1.5 \times 10^{-7}$	0.115	0.115	86640	<0.1	0.4
C4	$1.5 \times 10^{-6}$	0.930	0.930	576600	<0.1	0.1
C5	$1.5 \times 10^{-6}$	0.885	0.885	522150	<0.1	0.1
C6§†	$1.3 \times 10^{-6}$	0.613	0.307	72263	<0.1	0.5
C7§†	$1.4 \times 10^{-6}$	0.589	0.295	61950	<0.1	0.6
C8§*†	$1.2 \times 10^{-6}$	0.581	0.291	70325	<0.1	0.5
C9§‡	$2.3 \times 10^{-6}$	0.615	0.308	41111	<0.1	0.9
C10§‡	$2.8 \times 10^{-6}$	0.563	0.282	28301	<0.1	1.3
C11§‡	$1.5 \times 10^{-6}$	0.660	0.330	72600	<0.1	0.5
C12	$3.3 \times 10^{-7}$	0.914	0.914	2531503	<0.1	<0.1
C13	$4.9 \times 10^{-7}$	0.956	0.956	1865175	<0.1	<0.1
C14§†	$4.8 \times 10^{-7}$	0.669	0.335	932419	<0.1	<0.1
C15§†	$4.0 \times 10^{-7}$	0.689	0.345	296700	<0.1	0.1
C16	$1.0 \times 10^{-6}$	1.050	1.050	1102500	<0.1	<0.1
C17	$1.9 \times 10^{-6}$	0.986	0.986	511682	<0.1	0.1
C18	$5.5 \times 10^{-6}$	0.692	0.692	21766	<0.1	1.7

See Tables 1 and 2 for material composition; Table 3 for experimental boundary condition.  $H$  is deposit thickness;  $D$  is optimal diffusivity coefficient;  $L$  is characteristic length scale;  $\xi$  is the ratio of surge period to pressure-dissipation time; see text for definition.

§ Drained basal boundary; computation of characteristic diffusion time based on  $L = \frac{1}{2}H$ .

† Gravel substrate.

\* Uncompacted sand substrate.

‡ Compacted sand substrate.

nitudes of surface settlement indicate that dilated noncohesive slurries are highly compressible ( $C \sim 0.01$  kPa<sup>-1</sup>).

Depth-dependent excess fluid pressure, resulting from gravitational loading, drives transient fields of fluid pressure and effective stress that evolve upward from the base of a slurry rather than downward from the surface. This result is robust and holds regardless of basal boundary condition. Although a permeable substrate provides an additional pathway for fluid migration, gravity induces a nonsymmetric fluid-pressure field, and changes in sediment packing and fabric at the base of a deposit retard fluid loss. Basal textural changes, and an associated reduction of hydraulic diffusivity, during consolidation place significant limitations on mechanisms that affect debris-flow deposition. In particular, infiltration loss at the bed does not appear to be an important mechanism driving deposition.

Companion studies show that liquefaction pore-fluid pressure develops and persists during the brief lifetime of 10 m<sup>3</sup> experimental debris flows. The consolidation analysis presented here shows that such pore-fluid pressure does not dissipate substantially even over the lifetime of a typical natural debris flow. These results demonstrate that neither simple decay of excess pore-fluid pressure nor uniform viscoplastic yield strength can explain debris-flow deposition. Findings here bolster support for the hypothesis (Iverson 1997a; Major and Iverson 1999) that debris-flow deposition results from friction concentrated along flow margins where high pore-fluid pressure is absent.

Debris-flow deposits stabilize nonuniformly as effective intergranular stresses evolve upward from the base. Subsequent surges or flows can therefore remobilize strata irregularly if insufficient effective stresses are developed. Deposit remobilization may be preserved as soft-sediment deformation. However, deposit remobilization may simply mute or obliterate stratigraphic distinction among recurrent surges and flows and lead to a homogeneous deposit that appears to be the product of a single depositional wave.

#### ACKNOWLEDGMENTS

A collaborative study of debris-flow deposition with Richard Iverson stimulated the analysis of consolidation of debris-flow deposits. I am indebted to Dick for freely sharing his thoughts and criticizing my ideas during the course of the experiments. Both the flume and tank experiments could not have been completed without the support of Rick LaHusen, Tony Bequette, and Kevin Hadley. I appreciate their commitment to the success of this work. Fruitful discussions with Dick Iverson, Tom Dunne, David McTigue, Jim Vallance, and Evelyn Roeloffs focused my thoughts on consolidation and its geomorphic and sedimentologic significance. Tom Dunne, Dick Iverson, David McTigue, and Jody Bourgeois provided thoughtful criticisms of an early draft of this work. Evelyn Roeloffs, Joe Walder, Gerry Middleton, Marcus Bursik, and an anonymous reviewer provided insightful, critical reviews that

improved the final version. Any errors in fact or interpretation, however, are solely my responsibility.

#### REFERENCES

- AMERICAN SOCIETY FOR TESTING AND MATERIALS (ASTM), 1995, Annual Book of Standards: Soil and Rock standards D420-D4914, v. 4, no. 8, p. 197–206, 885–895.
- AUDET, D.M., AND MCCONNELL, J.D.C., 1992, Forward modeling of porosity and pressure evolution in sedimentary basins: Basin Research, v. 4, p. 147–162.
- BEEN, K., AND SILLS, G.C., 1981, Self-weight consolidation of soft soils: An experiment and theoretical study: Geotechnique, v. 31, p. 519–535.
- BIOT, M.A., 1941, General theory of three-dimensional consolidation: Journal of Applied Physics, v. 12, p. 155–164.
- BROSCOE, A.J., AND THOMSON, S., 1969, Observations on an alpine mudflow, Steele Creek, Yukon: Canadian Journal of Earth Sciences, v. 6, p. 219–229.
- CARRIER, W.D., III, BROMWELL, L.G., AND SOMOGYI, F., 1983, Design capacity of slurried mineral waste ponds: Journal of Geotechnical Engineering, v. 109, p. 699–716.
- CARSLAW, H.S., AND JAEGER, C.J., 1959, Conduction of Heat in Solids: Oxford, U.K., Oxford University Press, 510 p.
- CARTER, J.P., BOOKER, J.R., AND SMALL, J.C., 1979, The analysis of finite elasto-plastic consolidation: International Journal of Numerical and Analytical Methods in Geomechanics, v. 3, p. 107–129.
- CAS, R.A.F., AND LANDIS, C.A., 1987, A debris-flow deposit with multiple plug-flow channels and associated side accretion deposits: Sedimentology, v. 34, p. 901–910.
- COLLISON, J.D., AND THOMPSON, D.B., 1989, Sedimentary Structures: London, Unwin Hyman, 207 p.
- COSTA, J.E., 1984, Physical geomorphology of debris flows, in Costa, J.E., and Fleisher, P.J., eds., Developments and Applications of Geomorphology: Berlin, Springer-Verlag, p. 268–317.
- COSTA, J.E., AND WILLIAMS, G., 1984, Debris flow dynamics (video tape): U.S. Geological Survey, Open-file Report 84–606, 22 min.
- CRAIG, R.F., 1992, Soil Mechanics: London, Chapman & Hall, 427 p.
- CURRY, R.R., 1966, Observation of alpine mudflows in the Tenmile Range, central Colorado: Geological Society of America, Bulletin, v. 77, p. 771–776.
- DAVIS, E.H., AND RAYMOND, G.P., 1965, A nonlinear theory of consolidation: Geotechnique, v. 15, p. 161–173.
- DEGRAFF, J., 1994, The geomorphology of some debris flows in the southern Sierra Nevada, California: Geomorphology, v. 10, p. 231–252.
- ECKERSLEY, J.D., 1990, Instrumented laboratory flowslides: Geotechnique, v. 40, p. 489–502.
- EINSTEIN, A., 1906, Eine neue Bestimmung der Molekuldimensionen: Annalen der Physik, v. 19, p. 289–306.
- FOLK, R.L., 1984, Petrology of Sedimentary Rocks: Austin, Texas, Hemphill Publishing Company, 185 p.
- FOX, P.J., AND BERLES, J.D., 1997, CS2: A piecewise-linear model for large-strain consolidation: International Journal for Numerical and Analytical Methods in Geomechanics, v. 21, p. 453–475.

- FRYXELL, F.M., AND HORBERG, L., 1943, Alpine mudflows in Grand Teton National Park, Wyoming: Geological Society of America, Bulletin, v. 54, p. 457-472.
- GAMBOLATI, G., 1973, Equation for one-dimensional vertical flow of groundwater 2. Validity range of the diffusion equation: Water Resources Research, v. 9, p. 1385-1395.
- GHIBAUDO, G., 1992, Subaqueous sediment gravity flow deposits: practical criteria for their field description and classification: Sedimentology, v. 39, p. 423-454.
- GIBSON, R.E., ENGLAND, G.L., AND HUSSEY, M.J.L., 1967, The theory of one-dimensional consolidation of saturated clays—Finite nonlinear consolidation of thin homogeneous layers: Geotechnique, v. 17, p. 261-273.
- HAMPTON, M.A., 1979, Buoyancy in debris flows: Journal of Sedimentary Petrology, v. 49, p. 753-758.
- HICHER, P.Y., 1996, Elastic properties of soils: Journal of Geotechnical Engineering, v. 122, p. 641-648.
- HOOKE, R.L.E.B., 1967, Processes on arid-region alluvial fans: Journal of Geology, v. 75, p. 438-460.
- HOOKE, R.L.E.B., 1987, Mass movement in semi-arid environments and the morphology of alluvial fans, in Anderson, M.G., and Richards, K.S., eds., Slope Stability: New York, Wiley, p. 505-529.
- HUTCHINSON, J.N., 1986, A sliding-consolidation model for flow slides: Canadian Geotechnical Journal, v. 23, p. 115-126.
- INMAN, D.L., 1952, Measures for describing the size distribution of sediments: Journal of Sedimentary Petrology, v. 22, p. 125-145.
- IVERSON, R.M., 1997a, The physics of debris flows: Reviews of Geophysics, v. 35, p. 245-296.
- IVERSON, R.M., 1997b, Hydraulic modeling of unsteady debris-flow surges with solid-fluid interaction, in Chen, C.L., ed., Debris-Flow Hazards Mitigation: Mechanics, Prediction, and Assessment: American Society of Civil Engineers, Proceedings of First International Conference, San Francisco, California, August 7-9, p. 550-560.
- IVERSON, R.M., AND LAHUSEN, R.G., 1989, Dynamic pore-pressure fluctuations in rapidly shearing granular materials: Science, v. 246, p. 796-799.
- IVERSON, R.M., AND LAHUSEN, R.G., 1993, Friction in debris flows: Inferences from large-scale flume experiments, in American Society of Civil Engineers, Hydraulic Engineering '93, Conference, San Francisco, California, July 25-30 1993, Proceedings, p. 1604-1609.
- IVERSON, R.M., LAHUSEN, R.G., AND COSTA, J.E., 1992, Debris-flow flume at H.J. Andrews Experimental Forest, Oregon: U.S. Geological Survey, Open-file Report 92-483, 2 p.
- IVERSON, R.M., LAHUSEN, R.G., MAJOR, J.J., AND ZIMMERMAN, C.L., 1994, Debris flow against obstacles and bends: dynamics and deposits (abstract): EOS, Transactions of the American Geophysical Union, v. 75, no. 44, p. 274.
- IVERSON, R.M., REID, M.A., AND LAHUSEN, R.G., 1997, Debris-flow mobilization from landslides: Annual Review of Earth and Planetary Sciences, v. 25, p. 85-138.
- JAEGER, J.C., AND COOK, N.G.W., 1979, Fundamentals of Rock Mechanics: London, Chapman & Hall, 593 p.
- JAHNS, R.H., 1949, Desert floods: Engineering and Science Journal, v. 23, p. 10-14.
- JOHNSON, A.M., 1970, Physical Processes in Geology: San Francisco, Freeman, Cooper, 576 p.
- JOHNSON, A.M., 1984, Debris flow, in Brunsten, D., and Prior, D.B., eds., Slope Instability: New York, Wiley, p. 257-361.
- KIM, S.B., CHOUGH, S.K., AND CHUN, S.S., 1995, Bouldery deposits in the lowermost part of the Cretaceous Kyokpori Formation, SW Korea: cohesionless debris flows and debris falls on a steep-gradient delta slope: Sedimentary Geology, v. 98, p. 97-119.
- LAMBE, T.W., AND WHITMAN, R.V., 1969, Soil Mechanics: New York, Wiley, 553 p.
- LEE, K., AND SILLS, G.C., 1981, The consolidation of a soil stratum, including self-weight effects and large strains: International Journal of Numerical and Analytical Methods in Geomechanics, v. 5, p. 405-428.
- LOWE, D.R., 1982, Sediment gravity flows: II. Depositional models with special reference to the deposits of high-density turbidity currents: Journal of Sedimentary Petrology, v. 52, p. 279-297.
- MAJOR, J.J., 1996, Experimental studies of deposition by debris flows: process, characteristics of deposits, and effects of pore-fluid pressure [unpublished Ph.D. thesis]: University of Washington, Seattle, Washington, 341 p.
- MAJOR, J.J., 1997, Depositional processes in large-scale debris-flow experiments: Journal of Geology, v. 105, p. 345-366.
- MAJOR, J.J., AND IVERSON, R.M., 1999, Debris-flow deposition—effects of pore-fluid pressure and friction concentrated at flow margins: Geological Society of America, Bulletin, v. 111, 1424-1434.
- MAJOR, J.J., JANDA, R.J., AND DAAG, A., 1996, Watershed disturbance and lahars on the east side of Mount Pinatubo during the mid-June 1991 eruptions, in Newhall, C.G., and Punongbayan, R.S., eds., Fire and Mud—Eruptions and Lahars of Mount Pinatubo, Philippines: Quezon City, Philippine Institute of Volcanology and Seismology and Seattle, University of Washington Press, p. 895-919.
- MAJOR, J.J., IVERSON, R.M., MCTIGUE, D.F., MACIAS, S., AND FIEDOROWICZ, B.K., 1997, Geotechnical properties of debris-flow sediments and slurries, in Chen, C.L., ed., Debris-Flow Hazards Mitigation: Mechanics, Prediction, and Assessment: American Society of Civil Engineers, Proceedings of First International Conference, August 7-9, San Francisco, California, p. 249-259.
- MARTOSUDARMO, S.Y., AND JOHNSON, A.M., 1997, Ability of muddy debris to remain mobile at low flow rates, in Chen, C.L., ed., Debris-Flow Hazards Mitigation: Mechanics, Prediction, and Assessment: American Society of Civil Engineers, Proceedings of First International Conference, August 7-9, San Francisco, California, p. 454-463.
- MIDDLETON, G.V., AND HAMPTON, M.A., 1976, Subaqueous sediment transport and deposition by sediment gravity flows, in Stanley, D.J., and Swift, D.J.P., eds., Marine Sediment Transport and Environmental Management: New York, Wiley, p. 197-218.
- MOHRIG, D., WHIPPLE, K.X., HONDZO, M., ELLIS, C., AND PARKER, G., 1998, Hydroplaning of subaqueous debris flows: Geological Society of America, Bulletin, v. 110, p. 387-394.
- MOHRIG, D., ELVERHOI, A., AND PARKER, G., 1999, Experiments on the relative mobility of muddy subaqueous and subaerial debris flows, and their capacity to remobilize antecedent deposits: Marine Geology, v. 154, p. 117-129.
- MORTON, D.M., AND CAMPBELL, R.H., 1974, Spring mudflows at Wrightwood, southern California: Quarterly Journal of Engineering Geology, v. 7, p. 377-384.
- OKUDA, S., SUWA, H., OKUNISHI, K., AND YOKOYAMA, K., 1981, Depositional process of debris flow at Kamikamihori fan, Northern Japan Alps: Japanese Geomorphological Union, Transactions, v. 2, p. 353-361.
- PIERSON, T.C., 1981, Dominant particle support mechanisms in debris flows at Mt Thomas, New Zealand, and implications for flow mobility: Sedimentology, v. 28, p. 49-60.
- POLETO, M., AND JOSEPH, D.D., 1995, Effective density and viscosity of a suspension: Journal of Rheology, v. 39, p. 323-343.
- POSTMA, G., 1983, Water escape structures in the context of a depositional model of a mass-flow dominated conglomeratic fan-delta (Abrijoja Formation, Pliocene, Almeria Basin, SE Spain): Sedimentology, v. 30, p. 91-103.
- ROELOFFS, E.A., 1996, Poroelastic techniques in the study of earthquake-related hydrologic phenomena, in Dmowska, R., and Saltzman, B., eds., Advances in Geophysics, v. 37: San Diego, Academic Press, p. 135-195.
- ROSENBLUM, N.A., AND ANDERSON, R.S., 1994, Hillslope and channel evolution in marine terraced landscape, Santa Cruz, California: Journal of Geophysical Research, v. 99, p. 14,013-14,029.
- SCHIFFMAN, R.L., PANE, V., AND GIBSON, R.E., 1984, The theory of one-dimensional consolidation of saturated clays IV. An overview of nonlinear finite strain sedimentation and consolidation, in Yong, R.N., and Townsend, F.C., eds., Sedimentation and Consolidation Models: American Society of Civil Engineers Geotechnical Engineering Division Symposium, San Francisco, California, Proceedings, p. 1-29.
- SCOTT, K.M., 1988, Origins, behavior, and sedimentology of lahars and lahar-runout flows in the Toulte-Cowlitz River system: U.S. Geological Survey, Professional Paper 1447-A, 76 p.
- SHARP, R.P., AND NOBLES, L.H., 1953, Mudflow of 1941 at Wrightwood, southern California: Geological Society of America, Bulletin, v. 66, p. 1489-1498.
- SILLS, G.C., 1975, Some conditions under which Biot's equations of consolidation reduce to Terzaghi's equation: Geotechnique, v. 25, p. 129-132.
- SKEMPTON, A.W., 1960, Terzaghi's discovery of effective stress, in Terzaghi, K., From Theory to Practice in Soil Mechanics: New York, Wiley, p. 42-53.
- SPENCE, K.J., AND GUYMER, I., 1997, Small-scale laboratory flowslides: Geotechnique, v. 47, p. 915-932.
- TAKAHASHI, T., 1991, Debris Flow: Rotterdam, A.A. Balkema, 165 p.
- TERZAGHI, K., 1923, Die Berechnung der Durchlässigkeitsziffer des Tonen aus dem Verlauf der Hydrodynamischen Spannungsercheinungen: Akademie der Wissenschaften in Wien, Sitzungsberichte, Mathematisch-Naturwissenschaftliche Klasse, Part IIa, v. 132, no. 3/4, p. 125-128.
- TERZAGHI, K., 1943, Theoretical Soil Mechanics: New York, Wiley, 510 p.
- TERZAGHI, K., 1956, Varieties of submarine slope failures: Proceedings of Eighth Texas Conference on Soil Mechanics and Foundation Engineering, Special Publication 29, Bureau of Engineering Research, University of Texas, Austin, September 14-15, p. 3.1-3.41.
- TOORMAN, E.A., 1996, Sedimentation and self-weight consolidation: general unifying theory: Geotechnique, v. 46, p. 103-113.
- VALLANCE, J.W., 1994, Experimental and field studies related to the behavior of granular mass flows and the characteristics of their deposits [unpublished Ph.D. thesis]: Michigan Technological University, Houghton, Michigan, 197 p.
- VALLANCE, J.W., AND SCOTT, K.M., 1997, The Osceola Mudflow from Mount Rainier: Sedimentology and hazard implications of a huge clay-rich debris flow: Geological Society of America, Bulletin, v. 109, p. 143-163.
- WASSON, R.J., 1978, A debris flow at Reshūn, Pakistan Hindu Kush: Geografiska Annaler, v. 60A, p. 151-159.
- ZHANG, S., 1993, A comprehensive approach to the observation and prevention of debris flows in China: Natural Hazards, v. 7, p. 1-23.

Received 10 April 1998; accepted 8 April 1999.

#### APPENDIX 1: SOLUTIONS FOR PERMEABLE-BED ANALYSIS

Allowing fluid drainage at both the surface and the bed of a debris-flow slurry establishes zero-pressure conditions at each boundary; thus  $P_* = 0$  at  $z = 0$  and at  $z = H$ . Solution of Eq 9 subject to these boundary conditions and to an initial fluid-pressure condition of the form  $P_* = P_{*0}(1 - z/H)$  is accomplished using the standard method of separation of variables for solving partial differential equations. The solution, similar to one given by Carslaw and Jaeger (1959, p. 96) for an initial condition of the form  $f(z) = kz$ , is given by

$$P_* = 2P_{*0} \sum_{n=1}^{\infty} \frac{1}{n\pi} \sin(\lambda_n z) e^{-\lambda_n^2 D t} \quad (\text{A1.1})$$

in which

$$\lambda_n = \frac{n\pi}{H}$$

From this solution for excess pore-fluid pressure, expressions for effective stress and surface displacement are given by

$$\sigma_{zz}^e = -(\rho_s - \rho_w)(1 - \phi) \times g \left[ (H - z) - 2H \sum_{n=1}^{\infty} \frac{1}{n\pi} \sin(\lambda_n z) e^{-\lambda_n^2 D t} \right] \quad (\text{A1.2})$$

$$u_H = -\frac{1}{E_c} (\rho_s - \rho_w)(1 - \phi) \times g \left[ 2H \sum_{n=1}^{\infty} \frac{1}{n\pi\lambda_n} e^{-\lambda_n^2 D t} - \frac{H^2}{2} - 2H \sum_{n=1}^{\infty} \frac{1}{n\pi\lambda_n} \cos(\lambda_n z) e^{-\lambda_n^2 D t} \right] \quad (\text{A1.3})$$